Native defects in gallium arsenide

J. C. Bourgoin and H. J. von Bardeleben
Groupe de Physique des Solides de l'Ecole Normale Supérieure, Centre National de la Recherche Scientifique,[a] *Tour 23, 2 place Jussieu, 75251 Paris Cedex 05, France*

D. Stiévenard
Laboratoire de Physique des Solides, Institut Supérieur d'Électronique du Nord, 41, Boulevard Vauban, 59046 Lille Cedex, France

(Received 24 November 1987; accepted for publication 12 July 1988)

We describe information which has been obtained on point defects detected in various types of GaAs materials using electron paramagnetic resonance as well as electrical and optical techniques. From a comparison of their characteristics and those of simple intrinsic defects (As and Ga interstitials, vacancies and antisites) it is concluded that native defects are not simple intrinsic defects, with the exception of the antisites, but complexes formed by the interaction of such defects between themselves or with impurities. Particular emphasis is given to the As antisite complexed with an As interstitial, the so-called EL2 defect which plays a major role in the electrical properties of bulk materials. Differential thermal analysis, positron annihilation, and x-ray diffraction demonstrate that bulk materials contain a large concentration of vacancy-related defects and As precipitates located along dislocations which play the role of gettering centers. Presumably, bulk materials also contain other As clusters of various sizes although only the smallest ones (EL2) have been detected. All these As clusters are sources of As interstitials which play an important role in thermal treatments. As to semi-insulating materials, their electrical properties result mainly from the compensation between the double donor, called EL2, associated with the As antisite and the double acceptor ascribed to the Ga antisite.

I. INTRODUCTION

Very often, once they are fabricated, electronic devices and integrated circuits do not work as expected. A principal reason is the existence of defects in the bulk material, at surface and interfaces, which originate from the material itself or are produced during various steps of its technological processing. Indeed, defects play a major role in the electronic properties of semiconductor material because they interact with free carriers (acting as scattering centers, traps, and recombination centers), and their effect is non-negligible even when their concentration is very small compared to the free-carrier concentration. In fact, their effect will become more and more important as the scale of devices decreases and as more multilayer systems are used.

For this reason the identification and characterization of defects in semiconductors, as well as the understanding of their electronic and thermodynamical properties, is very important and remains an active field of research. This is particularly true in the case of GaAs. The behavior of active devices, usually made from thin layers on a semi-insulating substrate or embedded in it, is strongly sensitive to different types of defects. Defects at the interfaces, between the material and the encapsulating (passivating) layer can give rise to leakage currents; surface defects at the edge of a gate electrode can induce an artificial increase of the gate length leading to a decrease of gain with frequency. Defects in bulk material can produce fluctuations in the voltage threshold due to their inhomogeneous distribution, junction degradation under current injection and side or back-gating effects (i.e., a parasitic low-frequency transconductance between two electrodes sharing the same substrate).

Though surface and interface defects are directly related to device processing technology, it is not the case for the bulk defects. The nature and concentration of bulk defects is of course dependent on the technological processes to which the material has been submitted, in particularly thermal treatments and ion implantation, but their presence is mainly due to the existence of native defects and impurities; i.e., to the mode of growth. In practice, devices are realized on semi-insulating substrates, the insulating property of which is due to the compensation of residual shallow dopant impurities by deep levels associated with various defects[1] among which the most important is the so-called EL2 defect. In this review we shall describe the properties of these native defects and try to shed some light on their nature in bulk semi-insulating as well as in intentionally doped materials. We shall exclude from the discussion the cases of (i) isolated residual impurities which give rise to shallow or deep levels, and (ii) the substitutional donor impurity which gives rise to an additional resonant level in GaAs or to a localized state (the so-called *DX* center) in GaAlAs alloys. Both will be the subject of other reviews in this journal.[2,3] The defects we want to deal with are therefore intrinsic defects, namely vacancies, interstitials, and antisites in both the Ga and As sublattices, as well as complexes between themselves or with impurities. We shall see that interaction of these defects with dislocations will also have to be considered.

Before we examine native defects it is necessary to de-

[a] Laboratoire associé à l'Université Paris VII.

 0021-8979/88/210R65-28$02.40

scribe our knowledge of simple intrinsic defects: As and Ga vacancies (V_{As},V_{Ga}), interstitials (As_i,Ga_i), and antisites (As_{Ga},Ga_{As}). This will be done in Sec. III. A description of the properties of these defects is important in two respects. *First*, it illustrate the complexity of defect identification. Although they are the simplest, these defects already present a large variety of behavior such as the existence of several associated localized levels in the forbidden gap (i.e., different possible charge states depending on the position of the Fermi level), a large electron-phonon interaction leading sometimes to metastable states (i.e., two different lattice configurations for the same charge state) or bistable states (i.e., two different lattice configurations for two different charge states), strong lattice relaxation and distortion, and negative U character (i.e., a negative electron-electron repulsion energy). For a comprehensive description of defect properties, see Refs. 4 and 5. As a result, the defect characteristics which are deduced from experiment strongly depend on parameters such as the nature and concentration of the dopant, temperature, etc. *Second*, because a native defect is formed by the interaction of these simple intrinsic defects between themselves and impurities, one can expect that the knowledge of the behavior of its components will help to identify it. This will be illustrated in Sec. V in the case of the EL2 defect which was recognized as being a complex of an antisite As_{Ga} with an As interstitial once the properties of these simple defects were determined.[6]

Because of their complex behavior defects have to be detected and studied with a variety of techniques, each one providing a piece of information. It is only by the conjunction of several techniques that a complete picture of a given defect can be obtained and the defect hopefully identified. For this reason we shall first describe briefly in the next section the techniques used to study point defects in order to summarize the type of information they provide and to point out not only their advantages but also their limitations. Then, after the case of intrinsic defects has been examined (Sec. III), we shall describe the information that these techniques have provided on the native defects (Sec. IV) with a particular emphasis on the EL2 defect (Sec. V). We shall see that most of the simple intrinsic defects are reasonably well known and identified. As to native defects, only the antisites and the antisite-related defect EL2 are now identified and most of their properties understood. From a technological point of view, the knowledge we have on the EL2 defect could be considered sufficient since this defect is the dominant one in a picture of a material whose wanted, or unwanted, doping is partly or fully compensated. However, we shall see that there are other defects in large concentration: the Ga antisite, also present in As rich semi-insulating materials, which plays an important role in the compensation mechanism and other defects inhomogeneously distributed, which are not always detected by electronic techniques. Related to the presence of dislocations, these defects are important, especially in liquid-encapsulated Czochralski material which is heavily dislocated, because they can be the cause of an inhomogeneous distribution of the electrical characteristics and presumably play a large role in the variation of the electrical properties with heat treatments.

II. EXPERIMENTAL TECHNIQUES

A. Introduction

In principle, the full knowledge of a defect requires the following information: *first*, of course, the nature of the defect, i.e., its atomic configuration including the lattice distortion and relaxation around it; *second*, its associated energy levels E_T and wave functions ψ_T. From these quantities it is then possible to deduce all its electronic characteristics: cross sections for carrier trapping σ_c, optical cross sections σ_0 from which one can deduce its properties as a carrier trap, recombination center, diffusion center, and its optical properties (absorption and emission). In order to obtain such information one relies on the study of these properties from which one derives the defect's electronic characteristics. Thus, one uses classical techniques sensitive to the electronic properties: namely, electrical and optical techniques and electron paramagnetic resonance (EPR).

The thermodynamic properties of the defect, migration, and formation energies are deduced from defect behavior under thermal treatment (diffusion, quenching, annealing) which is monitored by one of the above techniques. However, recently a technique based on differential thermal analysis (see below), allowing the direct measurement of the energy liberated during a defect reaction, has been proposed.[7]

Among these techniques, EPR is in general the one most suited for providing a direct identification of a defect although, as we shall see, this is difficult in GaAs. The other techniques which can provide limited information on the nature of the defect are absorption on localized vibrational modes and positron annihilation. Consequently, one usually has to rely on additional indirect ways to identify a defect. These consist of monitoring the defect concentration versus various parameters such as stoichiometry, irradiation by various types of energetic particles (electron, neutrons, ions), and the nature and concentration of the doping impurities.

The aim of this section is not to describe in detail all the techniques of defect characterization (such a description can be found, for instance, in Refs. 4 and 5) but only to recall the type of information they provide, with their limitations, in the case of GaAs.

B. Electrical techniques

Resistivity and the Hall effect give the concentration n and the mobility μ of free carriers. The evolution of n with the temperature T can be analyzed to provide the degree of compensation; i.e., the concentration of defects which compensate doping impurities. On the other hand, the mobility $\mu(T)$ can reflect the concentration of neutral and ionized defects which scatter free carriers. It is a common practice to deduce the total impurity concentration from the influence of scattering by ionized impurities, and the routine assessment relies on "universal" curves which provide the mobility (at 77 K) versus the free-electron concentration and the ionized impurity conentration.[8] The role of defects is neglected. Although it is possible to take into account defect

scattering, it appears difficult if not impossible to sort out the influence of impurities from that of defects. In addition, scattering by dislocations and possible space-charge regions should perhaps be taken into account. As we shall see in Sec. VI, dislocations are surrounded by a heavily disordered region which gives rise to a space-charge region in doped materials and potential fluctuations which could affect the scattering.[9] Finally, mobility is not sensitive to dipoles, i.e, to paired defects such as donor-acceptor pairs. For instance, strong mobilities can be obtained in semi-insulating materials which contain relatively large concentrations of two defects: the EL2 defect associated with the double donor As_{Ga} and the double acceptor Ga_{As} (see Sec. V), presumably because they are paired. Thus, although important for device evaluation and determination of donor and acceptor concentrations, the two quantities n and μ do not provide very much information about defects.

Fortunately, there is a spectroscopic technique,[10] deep level transient spectroscopy (DLTS), which allows the determination of the concentrations and energy levels of each individual defect provided their energy levels are located on the right side of the Fermi level. This technique consists of an analysis of the temperature variation of the capacitance transient of a reverse-biased barrier (Schottky or p-n junction) when carriers, emitted from a filled trap into a band, leave the space-charge region) (see Chap. 6 in Ref. 5). In this way, majority-as well as minority-carrier traps can be detected and their profiles[11] determined in the region near the surface whose extension, typically up to few micrometers, depends on the free-carrier concentration. The defect energy levels are obtained as the slope of an Arrhenius plot of the logarithm of the emission rate (corrected for the temperature dependence of the carrier velocity and of the density of states in the band) versus the inverse of the temperature. The slope of this plot (the electrical signature of the defect) gives an apparent energy E_a which must eventually be corrected for the temperature dependence of the cross section σ_c (see below) to obtain the true energy level of the trap. The position of the defect energy level E_T can be deduced from the distribution of the occupied traps in the depletion region; the free energy G_T of ionization is obtained from the depth at which the defect level crosses the Fermi level.[12] Thus, once the variations of E_a and σ_c with temperature are known, it is possible to calculate the associated enthalpy and entropy.[13]

With this technique it is also possible to monitor the filling kinetics of a trap[14,15] and thus to obtain the carrier capture cross section σ_c. (Actually, with the exception of few particular cases,[16] one can get only σ_c for majority carriers in the case of majority-carrier traps and σ_c for minority carriers in the case of minority-carrier traps.) One additional feature of the DLTS technique is that the electrical excitation pulse which is used to fill the traps can be replaced by an optical pulse, thus allowing the measurement of optical cross sections σ_0 for the transitions between a trap and both bands to be made.[17]

Because of its simplicity the DLTS technique is widely used although, at times, the conditions of its validity are not observed. Several conditions must be fulfilled in order to insure that the analysis of the capacitance transient provide correct results. *First*, the width W of the space-charge region must remain constant as the emission proceeds, which requires the trap concentration N_T to be small compared to the free-carrier concentration n which defines W. When N_T/n is not small enough (typically lower than 0.1),[18] W varies as the emission proceeds and, since the capacitance transient is no longer exponential, an analysis based on the exponential character of the transient provides a shift in the signature of the defect, which gives an apparent concentration smaller than the real one and, eventually, spurious peaks in the DLTS spectrum. This is one of the reasons why the signature of the EL2 defect is seen to be slightly different in different materials[19] or in the same material whose surface has been treated differently[20] and to exhibit some scatter from author to author, for defects are often observed in unintentionally doped n-type materials with a concentration which is of the same order of magnitude (10^{16} cm^{-3}) as the free-carrier concentration[21] or even larger.[22] However, this problem can be cured by the use of constant capacitance DLTS. *Second*, the change of the emission rate with electric field, which increases with the doping concentration for a given applied bias, is also a factor which modifies the signature of a defect and causes its apparent concentration to decrease when the electron-phonon interaction is large enough to give rise to phonon-assisted tunneling emission. This is, for instance, the case of EL2 (Ref. 23) which explains[24] the sharp decrease of its apparent concentration for large free-carrier concentrations (2×10^{17} cm^{-3}) that is attributed to the annihilation of this defect by shallow donors.[25] Finally, the quality of the barrier can play a non-negligible role. A leakage current at the edge of the barrier, equivalent to a resistance in parallel to the capacitance, can reduce the measured capacitance and hence the apparent concentration; a resistive material introducing a resistance R in series with the capacitance C such that $RC\omega$ is not small compared to unity (ω is the frequency at which the capacitance is measured) modifies strongly the amplitude and shape of the spectrum[26] and can even change its sign. Moreover, interface states,present often in Schottky barriers, can produce additional spectra when the near surface region is explored.[27]

This technique, as well as other similar capacitance techniques (such as admittance spectroscopy,[28,29] photocapacitance, thermally stimulated capacitance), has been extensively applied in the case of doped materials and has produced a large amount of information on the defects they contain (see Secs. III and IV). The study of σ_c versus temperature T and of σ_0 versus the energy $h\nu$ of the excitation light has shown that the electron-phonon interaction often plays an important role on the properties of defects. The exponential variation of σ_c with T^{-1}, at least in a limited temperature range, associated with the activation energy ΔE,[30] is characteristic of carrier capture by the so-called multiphonon emission process.[31] Because of the general shape of the spectrum, a simple fit for σ_0 ($h\nu$) allows one to obtain the so-called Franck–Condon parameter, d_{FC}, independent of the energy position of the threshold for the transition (see Chap. 4 in Ref. 5). This parameter can also be determined from a study of the emission rate with electric field when the tunneling emission assisted by phonons is

strong enough.[32] The two quantities, ΔE and d_{FC}, define the configuration coordinate diagram of the defect, which is a way to visualize the electron-phonon interaction. This diagram is a graphical representation of the total energy E (the electronic energy plus the potential energy for nuclear motion; i.e., the vibrational term $\frac{1}{2} k Q^2$) of the defect on the assumption that it interacts with only one lattice coordinate Q. In the diagram represented in Fig. 1, curve 1 is related to a defect filled with an electron while curve 2 corresponds to an empty defect with the electron in the conduction band. Since ΔE can be viewed in the multiphonon emission capture process as the energy barrier that a carrier has to overcome to be trapped on a defect site (see Chap. 6 in Ref. 5), it is the difference in energy between the minimum A and the point B where curves 1 and 2 cross. Also d_{FC} is the difference between the thermal ionization energy (E_T) and the optical energy represented by the vertical transition CD. Thus, two of the three quantities d_{FC}, ΔE, and E_T are sufficient to define the diagram when the parameter k of the vibrational energy term is known.

The existence of this electron-phonon interaction has several important consequences on defect behavior. A defect associated with a localized energy level in the forbidden gap can be present with at least two different charge states in the material depending on the Fermi level position. (Often a defect exhibits several levels in the gap and hence more than two charge states.) Because of the electron-phonon interaction, the distortion and relaxation of the lattice which surrounds the defect changes with the charge state. This modification of the defect configuration can be so strong that it leads to two completely different configurations for two different charge states (bistability) or even for the same charge state (metastability as illustrated by the case of EL2, see Sec. V). To this change of configuration corresponds a change in the defect total energy; thus, formation and migration energies, which characterize defect behavior in thermal processes such as annealing and diffusion, are charge state dependent. This phenomenon has been extensively studied in the case of intrinsic defects.[33–35] Another consequence is the existence of defect enhanced annealing by carrier recombination.[36] This phenomenon, recognized early,[37] was first observed in GaAs for irradiated laser diodes in which the damage was recovered by current injection.[38] Lang and Kimerling[39] performed the first quantitative study using an intrinsic defect produced by electron irradiation (the so-called $E3$ level; see Sec. III) and concluded that the annealing rate is proportional to the rate of recombination of electron-hole pairs on the defect level. They argued that the driving effect is the liberation of phonons which occurs when the defect captures a hole, the so-called energy release mechanism,[36] because the activation energy for annealing drops to a value equal to the energy liberated by hole trapping, i.e., the hole ionization energy. However, a systematic study[40] has shown that this activation energy varies with injection conditions and can be considerably smaller than the hole ionization energy. Since this cannot occur for an energy release mechanism, it has been proposed that another mechanism associated with the alternative charge state changes that the defect undergoes under injection[41] is taking place. For the study of all these phenomena the DLTS technique presents unique advantages since it permits one to modify at his convenience the charge state of a defect and to monitor the behavior of injected minority carriers.

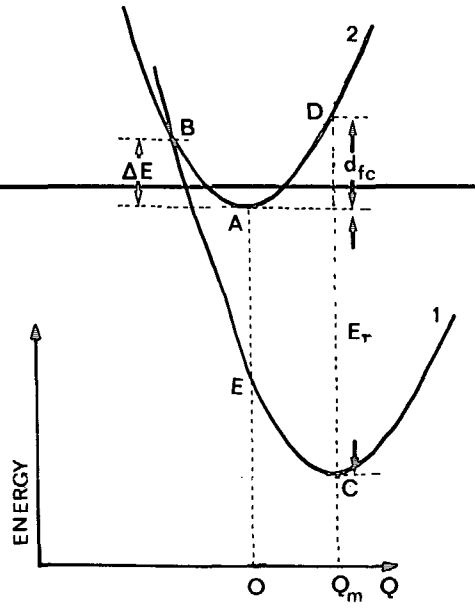

FIG. 1. Configuration coordinate diagram.

C. Optical techniques

Because of the electron-phonon interaction, the emission and absorption bands, corresponding to transitions $A \rightarrow E$ and $C \rightarrow D$, respectively, in the diagram of Fig. 1., are wide. An emission or absorption spectrum is not composed of a single line but of a band, centered around the A-E or C-D energies, which reflects all possible transitions between the vibrational states. For a strong enough defect-lattice coupling the vibrational contribution gives rise to a Gaussian line shape, determined by the parameters which define the configuration coordinate diagram (see Chap. 4 in Ref. 5), whose width increases with S, the Huang–Rhys factor $S = d_{FC}/\hbar\omega$, where $\hbar\omega$ is the energy of the phonon involved. Thus, because of the large electron-phonon interaction characterizing the defects in GaAs, the associated optical lines are very wide compared to the lines associated with shallow impurities and excitonic lines. The electronic part of the spectrum is often not easily recognized, the highest peak in energy of the band being not the electronic transition but a high-order phonon replica.

Consequently, emission and absorption spectra are only of limited use for the study of the electronic properties of deep levels. However, optical DLTS, which monitors optical absorption processes by an electrical technique, is a very convenient way to measure optical crosssections σ_0. The optical DLTS technique is based on an analysis of the kinetics associated with the return to steady state of the population of a defect under an optical excitation $h\nu$. Because of the general shape of a spectrum σ_0 ($h\nu$), this technique allows one to obtain independently the energy position for the threshold

of the transition and the Franck–Condon parameter (see Chap. 4 in Ref. 5). One additional, very important advantage of the capacitance technique over absorption is that it provides an accurate determination of the defect concentration.

However, optical techniques can be powerful in several cases. One is certain deep states which give rise to internal transitions unaccessible to electrical techniques; this is the case of the transition metal impurities for instance.[42] A second is deep levels which bind both electrons and holes simultaneously giving rise to bound-exciton recombination (undetected in optical DLTS); this is the case for complexes involving impurities such as Cu.[43] A third class of defects are donor-acceptor pairs. Excess carriers captured into donor and acceptor levels recombine radiatively. Usually, these levels are shallow but the same phenomenon can occur with deep states. The only illustrations we found for such deep donor-acceptor pairs in GaAs are described in Refs. 44 and 45. However, as we shall see in Sec.V, it is possible that As and Ga antisites coexist in pairs.

Finally, note that luminescence[46] has in principle a rather limited application for the study of deep levels because such levels usually act as nonradiative recombination centers, the carriers recombining, as we have mentioned above, through a multiphonon emission process. It is fortunate that, although deep, the EL2 defect does give rise to luminescence, a fact that could suggest that this defect is paired with an acceptor defect (see Sec. V).

D. Electron paramagnetic resonance (EPR) and related techniques

EPR is in principle the most powerful technique for defect identification because (see Chap. 3 in Ref. 5) (i) the central hyperfine structure of a spectrum, reflecting the interaction between the electron spin and the nuclear spin of the atom which composes the defect, can provide the nature of this atom; (ii) the superhyperfine interaction, reflecting the interaction of the electron spin with the nuclear spins of the atoms which surround the defect, provides the mapping of the defect wave function and information on its symmetry, extension in space, and thus the distortion and relaxation of the lattice around the defect. In GaAs, where all As and Ga atoms have a nuclear spin, the superhyperfine structure is generally not resolved and the lines are broad ($\sim$300 G). As a consequence the EPR spectrum is insensitive to the presence of weakly interacting defects. For instance, we shall see that the EPR spectra of the isolated antisite As_{Ga} and of the antisite complexed with an As interstitial are very similar. However, the application of an optical excitation can change the situation drastically. Superhyperfine interactions can be resolved by the electron nuclear double-resonance technique (ENDOR), in which the nuclear magnetic transitions of the nuclei coupled to the electron spin are detected through the variation of the saturated EPR signal. Because of much lower sensitivity of this technique as compared to EPR (several orders of magnitude), it has not been very often applied to GaAs.

The sensitivity of EPR is of the order of 10^{13} spins (for a linewidth of 10^2 G) and thus limited to the study of samples having mm^3 dimensions for typical defect concentrations of 10^{16} cm^{-3}. However, this sensitivity can be improved by optical detection (luminescence or absorption) which provides higher selectivity.[47] Electrical detection, such as that used to study spin-dependent recombination, could even be more sensitive than an optical detection.

E. Absorption by localized vibrational modes

High-resolution infrared absorption of localized vibrational modes is a powerful technique for detecting and identifying light impurities, isolated or paired, in semiconductors (see Chap. 5 in Ref. 4). It has been used in GaAs to detect light impurities[48] and to study the interaction defects with these impurities.[49] We do not detail this technique here like the Raman scattering technique, since they deal mostly with isolated impurities which we do not consider here.

F. Differential thermal analysis

The techniques described above provide the electronic characteristics of a defect. Its thermodynamic characteristics—total energy, migration energy, etc.—are deduced indirectly from the variation of their concentration during thermal processes such as migration, quenching, or diffusion. However, the energy stored by defects, as well as the energy involved in defect reactions, can be measured directly by a differential thermal analysis (DTA). In this technique, two samples of equal masses, the studied one and a reference sample, are submitted to a thermal scan inside a calorimeter. The difference between the heat power necessary to maintain the two samples at the same temperature during the scan gives the energy which is released in the defect reaction occurring in the studied sample (the reference sample has been submitted to an identical scan prior to the measurement). Typically, with a calorimeter having a sensitivity of the order of 10 mW, it is possible to detect the release of 10^{18} eV which occur in a 100 K range with a rate of 1–10 K min^{-1}. The validity of such a technique has been tested in GaAs on the recombination of As vacancy-interstitial pairs.[50] Indeed, these defects for which recombination kinetics are known (see Sec. III) can be created in a controlled concentration by electron irradiation and it is possible to compare the corresponding stored energy with the calculated one (see Fig. 2).

G. Positron annihilation

Positron lifetime increases when, before the positron annihilates with an electron of the material, it is trapped in a localized region where a nucleus is missing. Thus, the trapping rate is related to the concentration of vacancies or of any defect involving a missing atom, which we call a vacancy-related defect. Positron annihilation (PA) is now used for the study of defects in semiconductors but, from the large scatter in the results and sometimes conflicting results, it appears clear that the application of this technique in semiconductors is far more complicated than in metals.[51] These

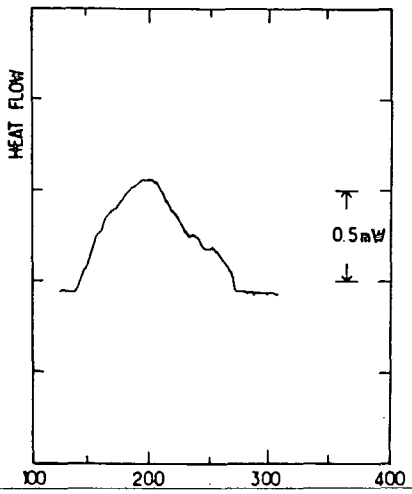

FIG. 2. Energy liberated by the recombination of V_{As}-As_i pairs in n-type doped (2×10^{18} cm^{-3}) GaAs with a temperature scan of 8 °C min^{-1}. These pairs being created by electron irradiation (1 MeV, 5.5×10^{17} cm^{-2}), their concentration is known and integration of the DTA curve allows the determination of the energy stored per pair (8.5 eV).

complications are a consequence of the fact that defects have several charge states in the forbidden gap and, once again, of the electron-phonon interaction.[52] Indeed, positron trapping is expected to vary with the defect charge state due to the positron-defect Coulomb interaction and thus to be strongly dependent on the Fermi-level position; i.e., to vary with the nature and concentration of the doping impurity and with temperature. In addition, the trapping rate reflects the mechanism by which the positron is trapped, a consequence, as we have discussed above, of the magnitude of the electron-phonon interaction, which is also temperature dependent. Finally, a large lattice distortion or relaxation can result in a non-negligible variation of the electron density at the defect site which further influences the positron annihilation rate.

Thus, although this technique has in the past provided some important information (see Sec. IV), PA studies have been performed in GaAs (Refs. 53–64) still cannot be understood in detail with reasonable confidence. For instance, the fact that no defect is detected by PA can be interpreted as indicating that the material does not contain any vacancy-related defects or that these defects are positively charged. The fact that the PA response varies with temperature can be a consequence of defect annealing but also of a change of the defect charge state as the Fermi level position moves.

H. Theory

Finally, one can ask the question, can a comparison between experimental characteristics, such as an energy level, and their values predicted by theory be used to identify a defect? The answer is no for a simple reason. The methods used so far to calculate the electronic structure of a point defect, based on the local density theory or on empirical tight-binding approximations (see Chaps. 3 and 4 in Ref. 4), are not yet sufficiently accurate. In recent years, the tight-binding methods, because they were empirical, have been practically abandoned in favor or the local density method. Unfortunately, the local density theory leads to a large underestimation of the energy gap (0.9 eV instead of 1.5 eV in GaAs) and perfect-crystal Green functions are determined using the local density eigenvalues and eigenvectors but with a shift Δ [the so-called "cissor" operator: 0.6 eV (Ref. 65) in GaAs] of the conduction band to produce the correct energy gap. Consequently, the predicted position of an energy level suffers the same drawback[66] since a defect wave function is built with combinations of valence and/or conduction-band states leading to an uncertainty $\pm\Delta/2$ in its energy position. In addition, the calculations so far undertaken, with the exception of the As antisite,[67] have not taken into account lattice distortion and relaxation, a phenomenon which is known in a simple case, like the vacancy in silicon, to shift the energy levels appreciably and split them. However, that does not mean that theory has been and is useless for defect identification. It can predict reasonably well quantities such as the energy difference between two adjacent levels of a defect as well as trends in defect behavior. It has also helped in understanding specific properties which *a priori* has appeared surprising on the experimental level.

There is general agreement that a simple tight-binding molecular description provides essentially a correct description for simple defects and allows one to understand the physical phenomena involved. This will be illustrated in Sec. V for the metastable state of EL2, a split interstitial configuration (for interstitial and substitutional impurities see Chap. 3 in Ref. 4). Consider the case of substitutional impurities which can give rise to shallow levels (the doping impurities, for instance) as well as to deep levels (the antisites for instance). Because such an impurity makes a tetracoordinated bonding with its neighbors, it produces A_1 and T_2 (triply degenerate) bonding and antibonding states and, depending on the value of the shift U in the sp^3 energy at the defect site (see Chap. 3 in Ref. 4), one or several of these levels can be located in the forbidden gap. For instance, the A_1 antibonding state is in the upper half of the gap for a donor defect and its depth, the localized character of the wave function, depends on the difference between the sp^3 average energy of the impurity and of the host atoms (U). One of these levels can eventually be shallow, i.e., close to the bottom of the conduction band and must then be treated in the framework of the effective mass theory (a substitutional impurity does not produce, as stated by Dow[68] the A_1, T_2 bonding and antibonding levels *in addition* to a shallow level). However, an impurity which can be treated by the effective mass theory can also give rise to a deep level in a particular case. Indeed,there is a series of hydrogenic states associated with each of the conduction-band valleys. The lowest-energy states are determined by the Coulomb potential; i.e., depend mainly on the band masses; but they can be significantly perturbed by the central potential which is characteristic of the impurity. In GaAs the 1s state derived from Γ is shallow, $\sim$5 meV deep. For impurities such as Si there is little, if any, perturbation of this state by the central cell. However, the 1s state derived from an L valley, because of intervally mixing, can be considerably deeper. As a result, when the L band is lowered (by pressure or alloying), a deep state appears in the gap. As we shall develop elsewhere[69] the existence of a DX center,[70] i.e., of a level linked to the L band is associated with

this phenomenon and not, as argued by Morgan,[71] by the existence of a large Jahn–Teller distortion.

I. Final remarks

None of the above techniques is able to provide a complete set of information necessary to identify a defect and to deduce its electronic and thermodynamic properties. Therefore, they must be used in concert, which often raises problems because it is not always possible to ascribe characteristics obtained by two different techniques to the same defect. The reasons for this are numerous. For instance, different techniques require different types of materials. Electrical techniques are applied on conductive doped materials while optical absorption and EPR require insulating materials; thus the defects are probed in different charge states. Also, different techniques can probe different regions of the materials. DLTS and luminescence probe a surface region while EPR and optical absorption are sensitive to the whole material. Electrical techniques probe only the conductive regions of a material; i.e., do not detect defects which aggregate and form insulating regions. A possible correlation of the characteristics obtained by different techniques consists of using an "annealing spectroscopy"; i.e., in monitoring defect thermal stability: when characteristics present an identical behavior during thermal annealing, they can reasonably be ascribed to a unique defect. Nonetheless, it can and does happen that several defects anneal together, due to their interaction with a common mobile species (this is the case in GaAs for the 200 and 450 °C annealing stages).

With the help of electrical and optical techniques and, in particular EPR, a reasonable number of simple point defects have been reasonably well identified. The reason is that there are additional indirect means for defect identification based, as will be illustrated in the following sections, on the variation of defect concentration with various conditions such as irradiation with energetic particles (electrons in particular), the degree of stoichiometry, and the nature of the doping impurity.

III. INTRINSIC DEFECTS

A. Introduction

The aim of this section is to review our knowledge of simple intrinsic point defects; namely, vacancies, interstitials, and antisites in both the As and Ga sublattices. Indeed, the first step towards the identification of native defects is to compare their electronic characteristics with those of intrinsic defects, then to determine by a comparison of their thermal behavior if they are an association of intrinsic defects with themselves or with impurities.

Thanks primarily to electron irradiation studies, most of these intrinsic defects have been identified. This is because it is possible to displace only one single atom with an incident electron by a proper choice of its energy, a choice which can be made once the minimum energy which must be transmitted to a lattice atom in order to produce a displacement, the so-called threshold energy, is known (see Chap. 8 in Ref. 5). In addition, because the type of interaction between the incident electron and a lattice atom is well understood, it is possible by a judicious choice of the direction of irradiation as compared to the crystallographic directions to displace the atoms of a given sublattice in a preferential way. The reason is the following: for irradiation with an energy close to the threshold energy, an atom is displaced in a direction parallel to the direction of the incident electron; i.e., with a recoil angle equal to zero. This recoil angle increases with the energy. It is therefore possible to distinguish between Ga and As displacements using the polar character of the [111] direction. Consider, for instance, an electron beam directed along the [111] As axis of the crystal. The probability of a displacement of a Ga atom along this direction will be small because, since all the bonds parallel to this particular direction are oriented from one Ga atom to one As atom, the nearest As atom obstructs its recoil path. On the contrary, the probability of a displacement of an As atom is large because the lattice is wide open in front of it. Thus, the anisotropy ratio of the defect introduction rate for irradiations in two opposite [111] As and [111] Ga directions provides immediately the nature of the displaced atom.[72]

The study of defects induced by electron irradiation of GaAs, which used resistivity and the Hall effect as a way of monitoring the total defect concentration[73–76] on the assumption that all the created defects were trapping free carriers, started very early. Significant results were obtained only in the 1970s (Refs. 77–80) with the advent of the DLTS technique. Because it is a spectroscopic technique it allowed the determination of the introduction rate of each individual defect, its energy level, and thermal behavior. However, most of the conclusions drawn from these preliminary experiments were later strongly modified when more quantitative and systematic studies (for a recent review, see Ref. 35) were performed. These studies have allowed a firm identification of Frenkel pairs as well as the vacancy, V_{As}, in the As sublattice and have provided information on the behavior of the As interstitial, As_i. Subsequent studies using EPR led to the identification of the isolated As antisite, As_{Ga}, and of the pair As_{Ga} complexed with the As vacancy. Although none of these defects turn out to be native defects, we shall see (Sec. V) that knowledge of their properties has been of considerable help in identifying the native defect EL2.

B. The As Frenkel pair

The DLTS technique is a well adapted tool for measuring the threshold energy for the atomic displacement, T_d, and the anisotropy ratio of the introduction rates for different directions of irradiation because it measures the defect concentration in a region 1–2 μm below the surface in which the loss of energy of the incident electron is negligible and its direction still preserved. As a result, it has been possible to measure the threshold energy[81] and its orientation dependence,[82] as well as the anisotropy ratio [82,83] for the [111] As and Ga directions, for most of the defects detected.

The results of these DLTS studies, which have been presented elsewhere[35] in a detailed fashion, can be summarized as follows. In n-type material five electron traps (labelled $E1$–$E5$; see Fig. 3) and two hole traps (labeled $H0$ and $H1$;

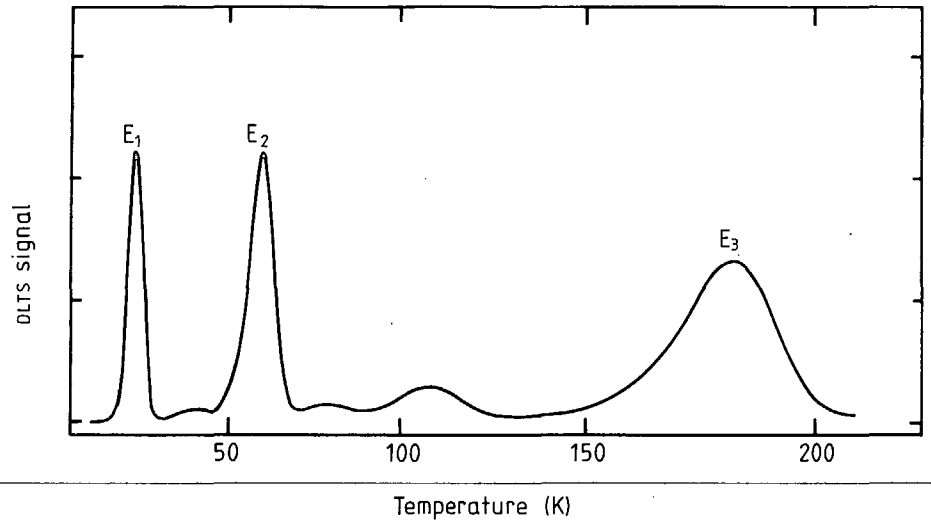

FIG. 3. Typical DLTS signal obtained in electron irradiated n-type GaAs, without minority-carrier injection, i.e., showing the majority-carrier (electron) traps. When the spectrum is recorded with the traps in the high electric field of the space-charge region the $E1$ and $E2$ peaks are strongly distorted and shifted towards lower temperatures.

see Fig. 4) have been detected which are associated with primary defects because (i) they are created at the lowest temperature (4 K), (ii) the sum of their introduction rates is of the order of the one calculated, with the value found for T_d, for primary displacements, and (iii) these defects are independent of the nature and concentration of the doping impurity as well as of the growth mode; i.e., the nature of the residual impurities and defects.

The variation of the anisotropy ratio performed for all these traps (except traps $E4$ and $E5$) demonstrate that these primary defects belong to the As sublattice (see Fig. 5). They are As Frenkel pairs, V_{AS}-As_i, because (i) they anneal together around 220 °C with a first-order kinetics and the annealed fraction is nearly 100%, which is characteristic of pair recombination[84] and (ii) the energy released per defect is that calculated for the recombination of a Frenkel pair.[50] The reason that a series of traps is associated with these V_{as}-As_i pairs is that, as can be seen from a careful examination of the end of the recombination kinetics, there is a distribution of the distances between V_{As} and As_i. Traps $E1$ and $E2$ correspond to two levels associated with different charge state transitions of the same defect,[35] the isolated vacancy V_{As}; i.e., the pair in which As_i is at several interatomic distances from V_{As}. Traps $E3$ and $E5$ correspond to pairs in which the As_i are near, probably at the third- and second-neighbor interstitial positions. The $H0$ and $H1$ traps correspond perhaps to other levels of the above defects. There is some evidence that the $E4$ trap is associated with the As_{Ga}-V_{As} complex.[85] In p-type materials the same electron and hole traps are observed[34]; i.e., the same defects are present. However, additional defects are also detected whose nature depends on the type of growth of the material.[34,86] These additional hole traps are attributed to complexes involving the interaction of primary defects with impurities. This conclusion implies a mobility of V_{As} or of As_i during the irradiation, which is larger in p-type than in n-type materials. The mechanism which induces such defect mobility in an electronic one; namely, the energy is provided by the recombina-

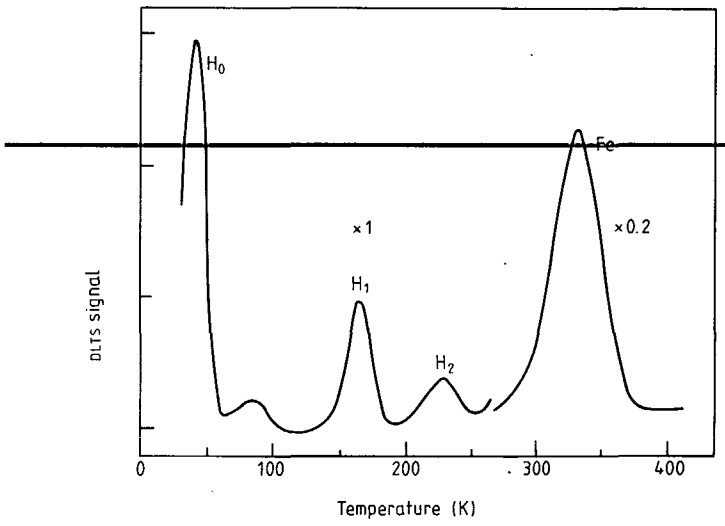

FIG. 4. Typical DLTS spectrum of the majority-carrier (hole) traps in electron irradiated p-type GaAs. This material contains before irradiation a native trap (Fe) associated with iron.

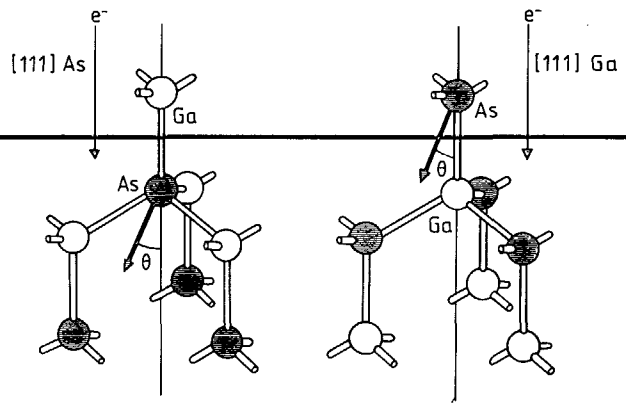

FIG. 5. In the zinc-blende structure of GaAs the (111) Ga and (111) As directions are, respectively, "hard" and "easy" directions for the displacement of an As atom (and conversely for a Ga atom) because a nearest-neighbor Ga atom is, or is not, in the direction in which the As atom recoils when the electron energy is chosen so that the recoil angle (θ) remains small. The anisotropy of the defect production rate when electron irradiation is performed in these two directions, thus tells the nature of the displaced atoms.

tion of carriers at the defect site (see Sec. II) as can be illustrated by using injection of minority carriers.[40] A direct evidence of such long-range migration is provided by the observation of the localized vibrational modes associated with B and C impurities; a fraction of these modes, increasing with the irradiation dose, shifts in energy because they are modified by the presence of a nearby defect.[87,89]

C. The As vacancy

Recently, the above description has been substantiated by EPR observations. A spectrum (Fig. 6) is observed under optical excitation in electron-irradiated material which is consistent with a V_{As} slightly perturbed by entities in interstitial second- and third-neighbors positions.[90] We have also recently observed this spectrum at thermal equilibrium in p-type material. The annealing process of this V_{As} defect has been monitored by EPR in semi-insulating material irradiated with a dose of 10^{17} electrons cm^{-2}. After such a dose, most of the Frenkel pairs have dissociated due to the long-range migration of the interstitial (see below). As a result, only a fraction of V_{As} anneal at 220 °C (see Fig. 7), a larger fraction disappearing well above this temperature (around 450 °C), a result verified by PA.[52] This demonstrates that it is As_i which becomes mobile and recombine with V_{As} in the 220 °C annealing stage.

D. The As antisite

The As antisite was first observed in semi-insulating GaAs using submillimeter EPR.[91] The spectrum (Fig. 8) consists of a set of four lines of equal intensity, implying it is due to a spin $S = \frac{1}{2}$ defect with hyperfine interaction with an $I = \frac{3}{2}$ nucleus (100%). The spectrum is isotropic. Due to this tetrahedral symmetry the defect must be a substitutional or an interstitial atom. This atom is As because impurities having the same nuclear spin cannot be involved[91]; thus the defect is an antisite or an As interstitial. The As_i configuration has been ruled out, as in the case of the P antisite in GaP, for charge state reasons. The best argument in favor of the antisite As_{Ga} is the thermal stability of the defect which is considerably higher than 220 °C, the temperature at which As_i becomes mobile.

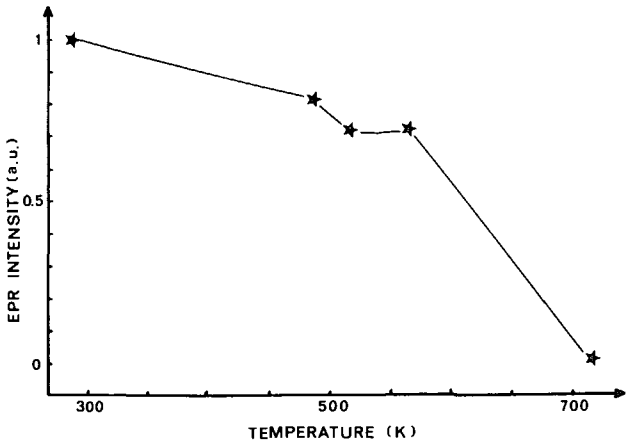

FIG. 7. Isochronal annealing of the As vacancy.

EPR has demonstrated that As_{Ga} are also formed during electron irradiation by two different mechanisms which are the consequence of the long-range migration of As_i (Ref. 92) which is possible when the time of irradiation is long. In n-type doped materials the variation of the antisite introduction rate versus the dose of irradiation[93,94] can only be understood by structural instability of V_{Ga} which transforms into the As_{Ga}-V_{As} complex; then the interaction of this complex with As_i leads to the formation of the isolated As_{Ga}. In semi-insulating materials this process is no longer effective since the As_{Ga}-V_{Ga} complex is not formed, but As_{Ga} are formed by the exchange interaction between As_i and substitutional Si giving rise to As_{Ga} and Si interstitials, a mechanism which is well known to occur in silicon.[95] Thus EPR allows us to verify that the entity which migrates under electron irradiation is As_i.

E. The As antisite–As vacancy complex

EPR detects (see Fig. 8) the Ga vacancy defect, which is unstable in n-type GaAs and transforms into the complex

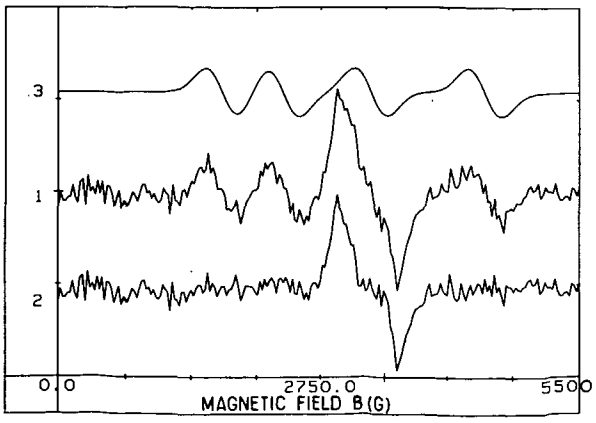

FIG. 6. Photo-EPR spectrum (1) observed in electron irradiated semi-insulating GaAs providing, after subtraction of the simulated (Breit Rabi) antisite spectrum (3), the spectrum associated with the As vacancy (2).

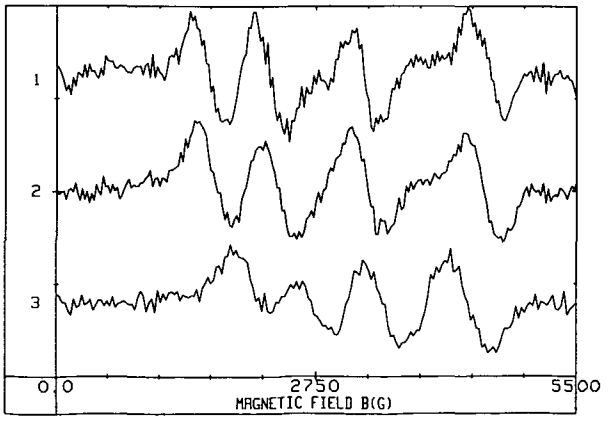

FIG. 8. Arsenic antisite related EPR spectra in as-grown semi-insulating (1) and electron-irradiated n-type GaAs, at the initial state (3) of irradiation (material remaining n type) and at a later one (2) (material becoming semi-insulating). The spectra correspond to the As_{Ga}-As_i complex (1), the isolated As_{Ga} and the As_{Ga}-V_{As} complex.

$As_{Ga} + V_{As}$.[96] It is this defect which we think corresponds to the $E4$ trap (it cannot be classified among the levels associated with Frenkel pairs because it has a different annealing behavior under minority-carrier injection). This observation is interesting because it therefore allows us to probe the mechanism by which this transformation happens and the stability of V_{Ga} as a function of the Fermi level, a question which will be important for the identification of the EL2 defect (see Sec. V).

F. The divacancy

To be complete, one should also mention that another defect is created by electron irradiation which anneals below room temperature (beteeen 235 and 280 K). First observed using conductivity measurements,[74] the defect was later detected by DLTS[35] and its level position determined[97] ($E_a = E_c - 0.23$ eV, $\sigma_a = 3\times10^{-14}$ cm^2). Because it is associated with a threshold energy about two times the threshold energy for a simple displacement, it has been suggested[81] that it is related to a double displacement; i.e., to a pair of vacancies $V_{Ga} + V_{As}$, a conclusion consistent with PA studies.[58]

G. The As interstitial

We now consider the question of the observation of interstitials. Interstitials are undoubtedly created by irradiation. Moreover, As interstitials are present after electron irradiation since we observe their recombination with vacancies at 220 °C. However, they are not detected directly either by EPR or by electrical or optical techniques. Their presence is only observed by the perturbation they produce on the EPR spectrum of the vacancy [in electron-irradiated GaAs (Ref. 90) and ZnSe (Ref. 98)]. This actually is a general problem for most semiconductors: although interstitials bound in a complex can be detected [this is, for instance, the case of Ga interstitials in GaAlAs (Ref. 99)] it has never been possible to observe an isolated interstitial in any semiconductor. (There seems to be, however, one exception[98] in a II-VI material.) The reason for this nonobservability could be the fact that such a defect has no state in the gap; i.e., it can exist in only one (nonparamagnetic) charge state. As argued by Lannoo,[100] the balance between electron-electron repulsion and lattice distortion may be such that only one stable state exists in the gap for this type of defect.

Fortunately, we have information on the thermodynamic behavior of the As interstitial through annealing kinetics. We have seen that the 220 °C annealing stage is related to the recombination of V_{As}-As_i pairs through the As_i mobility. This recombination involves two processes in series: the migration of the interstitial with migration energy E_m, and its jump into the vacancy over a barrier E_R once it has reached a neighboring vacancy site. Since kinetics are characteristic of the process which limits the reaction, the activation energy associated with the recombination kinetics, 1.5 eV,[34,84] should therefore be ascribed to E_m or E_R. We now turn to the annealing behavior of the complexes involving As_i observed in p-type material, the $H2$–$H5$ traps.[34] The kinetics is characterized by an activation energy of 0.51 ± 0.02 eV and a preexponential factor corresponding to a large number ($\sim 10^{10}$) of jumps. In this case the annealing process involves the breaking of the complex, characterized by a binding energy E_B, followed by As_i migration with energy E_m. Because this annealing is characterized by long-range migration, it is the last process which limits the reaction. Thus, the activation energy measured should be ascribed to E_m. It is therefore possible to recognize the existence of As interstitials through their migration energy $E_m \sim 0.51$ eV.

H. The Ga antisite

Materials grown in Ga-rich melts, which are p-type conductive, exhibit a photoluminescence peak at 1.44 eV (Ref. 101) whose behavior with temperature, excitation energy, and intensity indicates that it is related to an acceptor level located at 77 meV above the valence band. This level was later investigated extensively using the Hall effect,[102,103] photoluminescence,[101,103–106] infrared absorption,[105–107] DLTS,[103] and thermally stimulated conductivity.[108] Results of combined DLTS, photoluminescence, and the Hall effect showed that the defect responsible for this photoluminescence was actually a double acceptor with levels at 77 and 203 meV.[103] Peaks exhibiting infrared absorption (at 70.8, 72.9, and 74.5 meV) and which disappear above 50 K indicate transitions between the ground state and excited states associated with the 77 meV acceptor level.[107]

Because the concentration of these defects was found to exhibit a sharp increase with the boron concentration[102] and is directly related to the As fraction in the melt, decreasing when this fraction increases,[107] it was originally proposed that the defect responsible was a complex involving boron,[102] a Ga antisite complexed with an impurity,[101] or even an As vacancy.[107] However, because infrared spectroscopy shows that the defect has a T_d symmetry,[107] it was soon concluded that it could only be a Ga antisite or a boron on an As site, B_{As}, which is also a double acceptor. But local mode spectroscopy shows that boron is mostly substitutional on Ga sites and that B_{As} is not observed in p-type materials.[109] Moreover, there is no apparent correlation between the double acceptor and boron concentrations.[107] Thus, this double acceptor must be the Ga antisite.

Recently this defect was also observed, using photoluminescence, in MBE-grown material when the growth temperature is low enough and the stoichiometry corresponds to Ga-rich conditions.[110]

Finally, it has been argued[111] that this defect is responsible for the so-called FR2 EPR spectrum (Fig. 9) (see Sec. IV), observed in semi-insulating material, mostly because it appears after heating at 80 K temperature at which the ionization of Ga_{As}^{2-} into the paramagnetic state Ga_{As}^{-} occurs. The fact that this defect is present in a stoichiometric material will be discussed in Sec. V.

All the characteristics of these defects, energy levels, EPR parameters, optical transitions, Franck–Condon shifts d_{FC}, and activation energies ΔE associated with carrier capture cross sections are given in Table I.

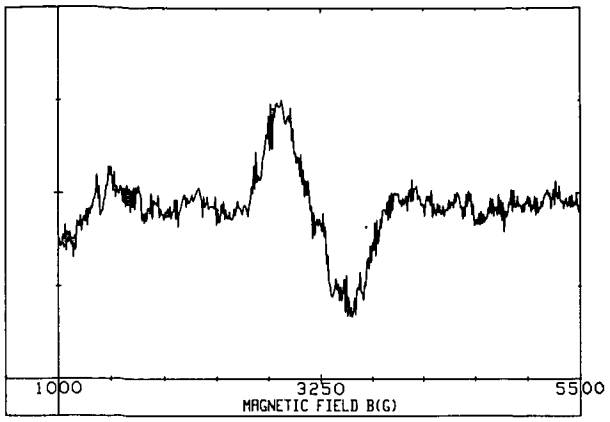

FIG. 9. Phot-EPR spectrum (FR2) in as-grown semi-insulating GaAs after EL2 quenching and 80 K thermal annealing.

I. Final remarks

There are other ways to create defects, namely, irradiation with particles other than electrons (neutrons, protons, heavy ions), plastic deformation, and quenching. However, these techniques do not create simple intrinsic defects. Irradiation with heavy particles produces cascades of displacements, i.e., disordered regions in which the defect concentration is very high, and the resulting defects are clusters of simple defects. Of course, at the edge of such disordered regions, simple intrinsic defects can exist in relatively small concentrations. As to plastic deformation and quenching, they necessitate the heating of the material to temperatures at which intrinsic defects are mobile (with possibly the exception of antisites). Consequently, they diffuse and interact with themselves or impurities, they getter on surfaces and dislocations, and the resulting defects are no longer simple intrinsic defects but complexes, some of which may occur as native defects.

Indeed, native defects can only result from interactions of intrinsic defects between themselves or with impurities during material cooling. Plastic deformation produces defects which have DLTS signatures identical to those of the native defects EL3, HL8, EL2,[114] EL6, and HL9[115] (see Sec. IV). The EPR spectrum of the As antisite is also produced[116] but it has not been verified that this antisite is an isolated one or is involved in a complex, such as EL2. In any case, this shows that antisite-related defects can be formed as a result of dislocation motion, a phenomenon which can occur at a reasonably low temperature in materials which are not too heavily dislocated or under current injection,[117,118] unless they are just revealed by a local change of the Fermi level around the dislocation.

Quenching gives in principle the formation energy of intrinsic defects which are at the origin of quenched defects. Lattice parameter measurements have given an energy of 2 eV,[119,120] but did not provide any information on the nature of the defects involved. The proposal of Potts and Pearson[121]

TABLE I. Characteristic properties of intrinsic defects as deduced from optical, DLTS (energy level E_i, measured from the bottom of the conduction band E_c or from the top of the valence band E_v, Franck–Condon shift d_{FC}, capture cross section $\sigma_c^{e,h}$ for electrons and holes, activation energy associated with the capture cross section ΔE), EPR characteristics (g value, hyperfine tensor A, crystal field splitting D, and electron S and nuclear I spins), and thermal stability (temperature, activation energy E associated with the annealing process).

Defect	Optical properties	DLTS	EPR	Thermal stability	References
V_{As}		$E1 = E_c - 0.045$ eV $(2-/-)$ $d_{FC} = 0.38$ eV; $E2 = E_c - 0.14$ eV $(-/0)$, $d_{FC} = 0.22$ eV, $\sigma_c = 1.2\times10^{-13}$ cm^2, $\Delta E \sim 0$.	$S = 1$, $g_\parallel = 2.00$ $g_\perp = 2.02$, $D = 0.04$ cm^{-1}.		35, 90, 112, 113
$V_{As} - As_i$		$E3 = E_c - 0.30$ eV, $d_{FC} = 0.2$ eV, $\sigma_c^h(330\text{ K}) = 4\times10^{-15}$ cm^{-2}, $\Delta E = 0.35$ eV, σ_c^e (166 K) $= 2\times10^{-18}$ cm^{-2}, $\Delta E = 0.08$ eV, $E5 = E_c - 0.96$ eV, $H0 = E_v + 0.06$ eV; $H1 = E_v + 0.25$ eV.		220 °C $E = 1.5$ eV (recombination)	14–16, 32, 34, 35, 113
As_{Ga}			$S = \frac{1}{2}$ $g = 2.047$, $A = 0.090$ cm^{-1}, $I = \frac{3}{2}$.	> 950 °C	92, 133
Ga_{As}	Luminescence (1.44 eV) IR absorption (70.9, 72.9, and 74.5 meV).	$E_v + 0.077$ eV $(0/-)$, $E_v + 0.230$ eV $(-/2-)$.			101, 103, 107
$As_{Ga} + V_{As}$		$E4 = E_c - 0.76$ eV $(+/2+)$ $\leqslant E_c - 0.35$ eV $(0/+)$.	$S = \frac{1}{4}$, $g = 1.97$ $A = 0.068$ cm^{-1}, $I = \frac{3}{2}$.		85, 96
As_i				~200 °C $E = 0.5$ eV (migration)	34

that it is an As vacancy is certainly not valid because the annealing behavior of the quenched defects they observed is different from the V_{As} one obtained by EPR observation (see Sec. III). One should then rely on theoretical estimates to justify this formation energy of 2 eV. The question of the evaluation of a defect formation energy is not simple (see Chap. 6 in Ref. 4). Recently,[122,123] some progress has been made with the use of the local density theory, a technique which usually provides realistic values for total energies of ground states. Its validity has been confirmed for the total energy of a $V_{As} - As_i$ pair: the calculated value[122] is within 20% of the enegy released in its recombination as measured by DTA.[51] The calculated formation energies of all the intrinsic defects[122] are in fact considerably larger than 2 eV (about 14 eV for V_{Ga} and V_{As}, 8 eV for As_i and Ga_i, 10 eV for Ga_{As}, and 9 eV for As_{Ga}). It is a situation similar to the one for Ge and Si where quenching provides formation energies which are considerably smaller than theoretical evaluations and values derived from self-diffusion (see Chap. 6 in Ref. 4).

One final way to produce defects, specific to compound materials, is to vary the stoichiometry. The most significant works based on this idea are that of Bublik *et al.*[124] and of Driscoll and Willoughby[119,125] who both measured density and lattice parameters of crystals grown from melts of variable composition. The result, which shows an excess mass per unit cell for an As fraction larger than 1.05 and a mass deficiency for a lower As fraction, implies in As-rich materials the existence of either As_i or As_{Ga} (or both). This very important conclusion can be verified directly or indirectly in several ways. As will be discussed in Sec. VI, As-rich materials contain As aggregates as evidenced by the presence of clusters of As atoms attached to line dislocations and the existence of the EL2 defect which (see Sec. V) is just a small cluster of six As atoms. The EL2 concentration increases with the As fraction in the melt,[126] or with the As pressure during Bridgman growth[127]; similarly it is smaller in epitaxially grown material[128–132] than in melt-grown materials. Very often these observations have been interpreted to indicate that EL2 is a defect related to a Ga vacancy (see Sec. V), which illustrates that one should be very cautious when using thermodynamical arguments in cases like this one which involve many unknown parameters (such as formation and binding energies, defect charge states, etc.) and where reaction rates are unknown.

IV. NATIVE DEFECT CHARACTERIZATION

A. Electrical techniques

As we have shown in Sec. II, the DLTS technique provides the concentration, energy level, and capture cross section of defects which are located below the Fermi level provided they capture carriers in a time shorter than the time during which the emission rate is recorded (typically lower than 100 ms). It therefore allows one to make a catalogue of all the electrically active defects present in a material which can be made *n* and *p* type. Such catalogues are given in Tables II and III for various types of studied materials. They give the apparent activation energy E_a (which is, as discussed in Sec. II, the sum of the ionization energy E_T and of the activation energy ΔE associated with the capture cross section) of the signature (emission rate e versus the inverse of the temperature T) of all the defects observed (electron and hole traps) as well as their apparent capture cross-section σ_a:

$$eT^{-2} = \gamma\sigma_a \exp(-E_a/kT),$$

with

$$\gamma = 2.3\times10^{20}\ \mathrm{cm^{-2}\,s^{-1}K^{-2}} \quad \text{for } n\text{-type materials}$$

and

$$\gamma = 1.7\times10^{21}\ \mathrm{cm^{-2}\,s^{-1}\,K^{-2}} \quad \text{for } p\text{-type materials.}$$

We have tried to keep labels which were given when the defects were reported for the first time. It has happened often that the same defect has been labeled differently several times, the reason being that its signature is recorded in a small temperature range and is sensitive to several factors (see Sec. II), providing slightly different values of E_a and σ_a.

As shown in Tables II and III (see the references in these tables) a large fraction of the observed traps appear to be characteristic of a single mode of growth, indicating that they cannot be simple intrinsic defects. Only one defect is consistently observed in practically all materials: it is EL2 and, as we shall see in the next section, is an intrinsic defect. In bulk (both Cz- and Bridgman-grown) *n*-type materials, two defects are always observed: EL2 and EL6 with concentrations in the 10^{15}–$10^{16}\ \mathrm{cm^{-3}}$ range. The EL6 defect can be in a higher concentration near the surface, depending upon the way this surface has been treated (polishing, etching). In epitaxial materials the defect concentrations are much lower, in the 10^{13}–$10^{14}\ \mathrm{cm^{-3}}$ range, and these concentrations can be varied in a controlled way through growth conditions (stoichiometry and growth rate). In vapor-phase epitaxy (VPE) materials, EL2 is always present with another defect, EL5 when the growth rate is large enough. In normal molecular-beam epitaxy (MBE) materials, i.e., As rich, several levels are consistently observed. Liquid-phase epitaxy (LPE) appears to produce the purest *n*-type material since, apparently, it does not contain any trap.[137] However, LPE and VPE layers contain a number of hole traps, in particular the B or HB2 trap, whose concentration is strongly influenced by growth conditions.[137,151] Most of these hole traps have been observed as minority carrier traps; i.e., in *n*-type materials. Several of them are undoubtedly associated with defects involving transition-metal impurities (HB1 with Cr, HB3 and HL3 with Fe, HB4 with Cu, and HL12 with Zn) since they are only observed when these impurities are introduced in the material (for a detailed study of the Cr and Fe associated traps, see Ref. 152).

Practically no systematic studies have been performed on these traps apart from looking occasionally at the influence of the growth conditions on their concentrations and to their possible appearance with the introduction of a given impurity. Consequently, none of them have been identified with the exception of EL2 (see Sec. V). Even their thermal

TABLE II. (a) Characteristics (apparent activation energy and capture cross section) of electron traps observed in different types of materials with their labels. (b) Characteristics (apparent activation energy and capture cross section) of hole traps observed (as majority-carrier traps in *p*-type materials or as minority-carrier traps in *n*-type materials) in different types of materials with their labels.

(a) Electron traps

Label	σ_a (10^{-14} cm^{-2})	E_a (eV)	Material	References
EL2 (A)*	10	0.82	VPE, bulk, MOCVD, LED (In doped)	134, 139, 140–142
EL3 (B)	10	0.57	VPE, LEC (In doped), bulk	134, 142
EL4	10^2	0.51	MBE, MOCVD	143, 144, 149
EL5 (C)	20	0.42	VPE, LEC (In doped)	134, 142
EL6	1.5×10^2	0.35	Bulk, MBE, LEC (In doped)	142, 149
EL8 (D)	0.8	0.27	VPE, MBE	135, 144
EL9 (E)	0.7	0.22	VPE	135
EL10 (F)	0.7	0.17	MBE, VPE	135, 144
EL12 (A′)	5×10^2	0.78	VPE, MBE, bulk	135, 146
EL14	5×10^{-2}	0.21	Bulk	149
EL16	4×10^{-4}	0.37	VPE	149
EI1	7×10^{-2}	0.43	VPE	136
EI2	1	0.19	VPE	136
EI3	2	0.18	VPE	136
EB1	3.5	0.86	LPE (Cr doped)	137
EB7	1.7	0.30	MBE	138
E	30	0.74	MOCVD	139
E	6.4	0.26	LEC (In doped)	142
E	1.5×10^3	0.42	MOCVD	143
M3*	3	0.61	MOCVD	147
M4*	1	0.31	MOCVD	147
EA2	5×10^{-2}	0.52	bulk	150
EA6	/	0.18	bulk	150
EA7	0.1	0.14	bulk	150

(b) Hole traps

Label	σ_a (cm^{-2})	E_a (eV)	Material	References
HT1	1×10^{-14}	0.44	VPE	154
HS1	2×10^{-19}	0.58	LPE	155
HS2	4×10^{-16}	0.64	LPE, VPE	155
HS3	5×10^{-18}	0.44	LPE	155, 142
HB1	5×10^{-16}	0.78	LPE, VPE	137, 151, 157
HB2 (B)	1×10^{-14}	0.71	LPE, VPE	137, 151
HB3	3.5×10^{-16}	0.52	LPE, MBE	137, 151
HB4	3.5×10^{-14}	0.44	LPE, VPE	137, 151
HB5 (A)	2×10^{-13}	0.40	LPE, bulk	137, 151
HL3	3×10^{-15}	0.59	VPE	151
HL6	5.5×10^{-14}	0.32	VPE	151
HL7	6.5×10^{-15}	0.35	MBE	151
HL12	1.3×10^{-14}	0.27	LPE	151
H		0.57	MOCVD	143
HA6	2×10^{-14}	0.18	bulk	156

TABLE III. Characteristics of the EPR spectra observed in bulk materials.

Label	Characteristics	Remarks	References
EL2 (As_{Ga})	$g=2.04$, $A=0.089$ cm^{-1}	Photoquenchable at 1.1 eV	160
FR3	$g_{\parallel}=2.11$, $g_{\perp}=2.89$, $J=1/2$ or $3/2$	$Ga_{As}^{-}-B_{Ga}^{0}$ (?) under photoexcitation	161
/	$g=1.85$	after $T\geqslant450$ °C As_i complex (?) under photoexcitation	165
FR1	$g_{(100)}\simeq1.96$	under photoexcitation	162
FR2	$g=2.09$	Ga_{As}^{-} under photoexcitation	111, 162

stability, although important for applications, has not been systematically studied. In epitaxial layers defects are at least stable up to the growth temperature, i.e., ~500 °C, and their concentration too small to be a nuisance. However, it can happen that thermal treatment under particular conditions introduces a defect in a non negligible concentration; this is apparently the case for EL2 in MBE layers heated above 800 °C under a Si_3N_4 encapsulant.[146] In bulk materials in which the defect concentration is large, thermal stability has been probed but only for a few thermal treatments: typically at a temperature of 850 °C, used for annealing implanted damage, and sometimes at 450 °C, the temperature at which the Si_3N_4 encapsulant is usually deposited. The reported results obtained are not always identical because the DLTS

technique measures a concentration in a region close to the surface where it can vary sharply in a manner which depends on the encapsulation conditions and significant changes in concentrations for a 450 °C treatment have already been reported; at 850 °C all the defects have disappeared with the exception of EL2, whose bulk concentration does not change significantly. The same appears to be valid in In-doped materials although the concentration of EL5 is reported to increase following a 850 °C treatment.[142] There are only a few reports on the growth of new defects following a 850 °C treatment; Henini *et al.*[157] detected three new electron traps at 0.14, 0.35, and 0.44 eV below the conduction band but they did not indicate their corresponding concentrations; Reynolds *et al.*[158] reported the appearance of a photoluminescence line at 1.51 eV which they attributed to a donor–acceptor-type complex.

Among all the defects reported, only EL2 and the couple M3-M4 exhibit a metastable character. The case of EL2, being described in detail in Sec. V, we just note here that the behavior of the M3-M4 trap does not have the character of stable-metastable states as stated by the authors[147] but rather the character of a bistable defect. The presence of one or the other of these traps depends on the bias applied during cooling; i.e., of the charge trapped on the defect at low temperature. This behavior is typical of the one observed in Si for paired defects in Coulomb interaction.[159]

B. Electron paramagnetic resonance

This technique detects a series of defects (see Table III). The first one[160,161] has the signature of the As antisite (see Sec. III) and it has been demonstrated (see Sec. V) that is directly correlated to the presence of EL2. Its concentration is variable from sample to sample because, since it is observed in semi-insulating materials, the fraction of the population of this defect in the paramagnetic state varies with the Fermi-level position; this can be verified using band-to-band optical excitation.

Three other spectra, labeled FR1–FR3, have also been reported[162] which presumably compose the broad signal in the $g = 2$ region observed previously.[163,164] Not much is known about the two first spectra (FR1 and FR2) since it has not been possible to resolve the angular dependence of their components. They are seen under photoexcitation with the maximum of their spectral dependence not far from 1.1 eV, the energy of the intracenter transition for the quenching of EL2 (see Sec. V); in addition, they disappear with thermal recovery at 80 and 120 K, respectively, i.e., for temperatures close to the two stages at which the regeneration of photoquenched EL2 occurs. This indicates that charges are exchanged between EL2 and these two defects. However, recently it has been proposed[111] that the FR2 spectrum must be attributed to Ga_{As}. This spectrum has a particular line shape, indicating nonresolved hyperfine interaction comparable to the width of the individual lines, which can be modelized by a Ga_{As}^{-} defect. It appears at the temperature for which the transition from the 2 − to the − state takes place. The presence of this defect and of its ionization has been verified by optical absorption which allows one to monitor the concentration of Ga_{As} (through its electronic spectrum) and of the shallow acceptor impurities (through their localized modes of vibration). The third EPR spectrum (FR3), also detected (only at 35 GHz) under optical excitation, FR3 (161), is seen in liquid-encapsulated Czochralski (LEC)-materials when the encapsulation is made with boron nitride (BN) but not with silicon oxide nor in horizontal Bridgman (HB) materials. For this reason, it is tentatively assigned to a complex involving boron. Indeed LEC materials which are BN encapsulated contain boron in a wide range of concentration (10^{14}–10^{18} cm^{-3}) while the other materials are boron free. Because the spectrum is of trigonal symmetry ($g_{\parallel} = 2.11$, $g_{\perp} = 2.89$) and compatible with a p^5 configuration, Kaufmann *et al.*[161] suggest that this defect is a complex involving a neutral boron atom on a Ga site on the nearest-neighbor substitutional site of another entity, possibly the Ga antisite.

Finally, a new spectrum has been detected under photoexcitation[165] in materials thermally annealed (above 450 °C). Since the intensity of this spectrum follows the electric field distribution of the cavity, it involves probably an electric rather than a magnetic dipolar transition like the FR1 defect. It is thought to be associated with a complex involving an As interstitial formed when these interstitials are liberated in the 450 °C annealing state (see Sec. VI).

C. Optical techniques

As discussed in Sec. II, the detection of deep levels (except for the case of isolated transition metal impurities which, being introduced intentionally, are beyond the scope of this review) by optical absorption techniques is not sensitive because of the large linewidths, a consequence of the electron-phonon interaction. Optical absorption in bulk materials gives rise in the near infrared to a large band extending from 0.8 eV to the conduction-band edge. Because this band reproduces the photoionization cross section for electrons of the defect level EL2 obtained by optical DLTS and because it has identical photoquenching properties (see Sec. V), it has been attributed to transitions between the EL2 level and the three minima Γ, L, and X of the conduction band. However, infrared wavelength modulation absorption spectroscopy, because of its higher sensitivity, is able to detect other absorption spectra,[166] in particular, resonant peaks with fine structures near 0.37 and 0.40 eV (the first one being interpreted as an intracenter transitions between iron levels). In addition, this technique shows that an appreciable fraction ($\sim$20%) of the absorption band between 0.6 and 1.5 eV is due to defects other than EL2.

Photoluminescence associated with deep levels is observed in all n-type, but rarely in p-type, bulk materials. As discussed in detail in Ref. 167 the most common luminescence line in n-type materials, which occurs at 1.2 eV with a half width of 0.2 eV at 80 K, is believed to correspond to the recombination between a paired donor-Ga vacancy. That the defect involves a donor appears clear from excitation spectroscopy because of the variation of the emission peak energy with the nature of the donor. However, the nature of the deep level is not certain: it is derived from stoichiome-

try[168] and impurity solubility considerations[169] which are only indirect indications on the existence of an isolated V_{Ga} or of a V_{Ga}-related defect. When doped with *p*-type impurities the materials exhibit, in addition to the band-acceptor recombination, a line at 1.37 eV for group II impurities[170] and at 1.45 eV for group IV impurities[171] which have properties similar to the above complex and which also correspond to an acceptor-donor pair recombination where the donor is assumed to be the As vacancy. But again the evidence for the existence of an As vacancy is weak. The band in the 0.62–0.68 eV range is attributed to EL2 and discussed in Sec. V.

D. Differential thermal analysis

After the validity of this technique had been verified by measuring the energy released in the recombination of As vacancy-interstitial pairs,[50] it was used[7] to characterize bulk (LEC semi-insulating and highly Si-doped HB) materials by looking for defect reactions in the range 300–600 °C. A large release of energy ($\sim 10^{19}$ eV cm^{-3}) is detected around 450 °C in HB materials but not in LEC materials. From the shape of the DTA curve it is possible to determine the activation energy associated with the reaction if one assumes that the corresponding kinetics are first order. Because the fit is not very sensitive to the preexponential term (which should be of the order of 10^{12} s^{-1}) this activation energy (2.3 eV) has been obtained with a reasonable accuracy. Since the maximum energy which can be released by a defect reaction is ~ 8 eV,[50] the energy stored in a vacancy interstitial pair, it is possible to estimate the minimum defect concentration which gives rise to the DTA peak; it is $\sim 10^{18}$ cm^{-3}.

The presence of such a high defect concentration is *a priori* surprising since the techniques described above detect only defects in the 10^{16} cm^{-3} range. However, as we shall see below, the order of magnitude of this concentration is confirmed by PA studies. As developed in Sec. VI, the existence of such a high concentration is explained in the following way: when the dislocations become mobile they dissolve As clusters attached to them, allowing the As interstitials thus produced to recombine with the vacancy-related defects (detected by PA) which are also present along dislocations. The reason this process does not occur in LEC material is due to the fact that in this material the dislocations cannot move, their density (10^4–10^5 cm^{-2} EPD) being considerably higher than in HB material (10^2–10^3 EPD).

E. Positron annihilation

The PA technique has been used to characterize various types of bulk materials.[53,54,56,58,60–63] As expected (see Sec. II) from the fact that the positron trapping rate depends on several parameters (in particular, temperature, concentration, and nature of the impurities) the results obtained exhibit apparently large differences. This variety in the observed behaviors is well illustrated in Ref. 63 which provides positron trapping rates for various types of doping. Vacancy-related defects are usually detected, but not always in *p*-type[53,63] materials. Recognizing the effect of the Fermi level, the authors do not give an evaluation of the defect concentration in most cases. Whenever this evaluation can be done, i.e., in strongly *n*-type doped materials in which the defects are filled, the order of magnitude of the measured defect concentrations estimated are 10^{18} cm^{-3} and 1–4×10^{17} cm^{-3} (Refs. 54 and 63), both values for highly doped materials. This result is important because it confirms the observation of a high defect concentration made by DTA. The thermal stability of these defects is also the same as the one derived from DTA, namely, the existence of an annealing stage around 450–500 °C.[54,61–63]

V. THE EL2 STORY

A. Introduction

By using a transient capacitance technique, the existence of the main defect present in *n*-type material was detected quite early[172–175] as a donor state lying in the middle of the forbidden gap. The unusual behavior of the material, namely a persistent quenching of the photoconductivity at low temperature, was discovered only 10 years later.[176–177] The level associated with this defect was then rediscovered by DLTS[178] and labelled 0 or EL2. It was demonstrated that the above unusual behavior was caused by the presence of this level[179,180] and could be explained by the existence of a metastable state (i.e., of a second configuration of the defect, associated with the same charge state as the stable configuration) of the associated defect.[181] Because of this interesting physical behavior and because of its technological importance, since it was recognized that this defect was responsible for the semi-insulating character of undoped LEC material,[1] this defect was then extensively studied and its electronic characteristics determined.[182]

In principle it is easy to ascribe a given property detected in the material to the EL2 defect using the special fingerprint that represents this metastability. The defect is quenched, i.e., "disappears," by photoexcitation at 1.1 eV at low temperature and is regenerated by a thermal treatment at 140 K. This quenching corresponds to the transformation of the stable state of the defect into another one which is metastable since at a low enough temperature the defect remains in this new state after the optical excitation has been removed. However, in practice this is not so easy because there can be electron and hole transfer between other defects and EL2 during quenching and regeneration. For instance, the transformation of the stable into the metastable state takes place for one particular charge state only and, for this, electrons from ionized acceptor levels are metastably transferred to EL2. As a result, a proposed correlation between EL2 and a given property is sometimes found later to be only indirect, or a real correlation (the intracenter transition contained in the EL2 optical absorption) is rejected[183] after first being claimed[184] by the same authors.

The microscopic structure of this defect remained unidentified until recently. Models were proposed based on various types of configuration coordinate diagrams, all illustrating that a large lattice relaxation of the stable state was necessary to explain its metastable character and to show the coherence of its various electronic and optical characteris-

tics. First, it was thought that EL2 was related to oxygen because the incorporation of O results in high-resistivity materials[185] but careful studies in various types of materials demonstrated that there was no correlation between the EL2 concentration and the O concentration.[186–188] Numerous studies were then undertaken in order to determine its thermal stability, its introduction rate as a function of various parameters such as stoichiometry, doping concentration, its spatial distribution, and correlation with the presence of dislocations, which have brought important technological information but did not allow a significant progress concerning its identification. The first step towards the EL2 identification came with the EPR detection of the spectrum associated with the As antisite (see Sec. III) and the demonstration that this spectrum has the same metastable behavior as EL2.[189,190] At that time, atomic models started to fluorish all based on this observation: the isolated As_{Ga},[191] the pair of As_{Ga},[192] and the Ga vacancy[193] [because it could transform into a complex of As_{Ga} and V_{As} (Ref. 194)], a complex involving As_{Ga} and vacancies.[195–197] Only when systematic studies using combined EPR and DLTS were performed on materials which had been submitted to various treatments (electron irradiation, annealing, and quenching) has a significant step towards this identification occurred.[6,198] It was recognized that EL2 was a complex involving As_{Ga} and an interstitial entity which can be dissociated, revealing the thermal behavior of this interstitial. Because this behavior appeared to be very similar to that of As_i (see Sec. III), it was proposed[198] that the stable state of EL2 is the complex $As_{Ga}^{0/+}$ with As_i in the second-nearest-neighbor position, while in the metastable state As_i is in a position closer to As_{Ga} because the As_{Ga} EPR spectrum is only slightly perturbed for the stable state and disappears when EL2 is in its metastable state. This proposal was then verified directly by optically detected ENDOR spectroscopy[199] which provided the ligand hyperfine structure of this defect. This verification illustrated the potential of optical detection of ENDOR (ODENDOR) but also the complexity of the ligand hyperfine structure in GaAs. The authors first deduced from optical detection of EPR that As_{Ga} was not related with EL2[200] and from ODENDOR that several species of As_{Ga}-related defects were present.[201] When it was finally recognized that EL2 was a complex involving As_{Ga} and an interstitial, the interstitial involved was first thought to be a Ga one,[202] then As_i^-,[203] and finally As_i^+.[204]

The story of the identification of this defect is not yet over in particular because the character of the metastable state is still not understood. Up to now all attempts to identify it experimentally have failed which suggests that the defect has no associated gap state. Very recently it has been proposed on theoretical grounds that this state is an As split interstitial pair configuration.[205,206] Apparently, this configuration fulfills all the requirements necessary to explain the behavior and properties of the metastable state. However, a direct experimental verification is still lacking.

B. Electrical and optical characteristics

The characteristics of the main electron trap associated with EL2 has been obtained using DLTS. Its signature, when derived from correct conditions, i.e., in an n-type doped material whose concentration is at least 10 times larger than the EL2 concentration and in the low electric field region of the space-charge region, provides an apparent activation energy $E_a = 0.82 \pm 0.01$ eV and an apparent carrier capture cross section of $1.5 \pm 0.5 \times 10^{-13}$ cm^2.[207] The capture cross section for an electron σ_n has been directly measured[152] in a rather large temperature range (50–270 K).

$$\sigma_n = 5\times 10^{-19}(\text{cm}^2) + 6\times 10^{-15}(\text{cm}^2)\exp[-0.0566\ (\text{eV})/kT]$$

and the results show that it is thermally activated; i.e., the capture occurs by a multiphonon process which indicates the existence of a non-negligible lattice distortion. This is consistent with the variation of the emission rate with the electric field[207]: for high enough electric fields (larger than 10^5 V cm^{-1}) the emission rate is increased by phonon-assisted tunneling[208] and yields the Huang–Rhys factor $S = 6 \pm 0.5$, with $\hbar\omega = 20 \pm 5$ meV,[23] which characterizes this lattice distortion. The hole cross section has been evaluated to be $\sigma_p = 2\times 10^{-18}$ cm^2.[152] By using the variation of σ_n with T, it is possible to deduce the exact energy level position, $E_T = E_c - 0.76 \pm 0.01$ eV, and the associated entropy term, $S_T = 2.4\times 10^{-4}$ eV K^{-1}.

The electron and hole photoionization cross section have been measured by optical DLTS.[17] The spectral shape of the electron optical cross section reflects directly the density of states in the conduction band, i.e., the transitions to the Γ, L, and X minima are well resolved. This allows a fit to determine the threshold (ionization energy) and the Franck–Condon parameter d_{FC} (120 meV) which agree, within the experimental accuracy, with the above values derived from DLTS.

The nature, donor or acceptor, of this level has been determined by taking advantage of the profile the defect exhibits near the surface after a thermal treatment. The comparison of the defect profile and the free-carrier profile when the defects are empty or filled allows one to conclude immediately that the defect is a donor.[209] For this reason it has been widely assumed that the defect is neutral when filled and positively charged when empty. However, its charge could also be singly positive when filled and doubly positive when empty, this would be in agreement with the suggestion of Walukiewicz *et al.*[210] that there is a shallow donor state, 20–30 meV below the conduction band, associated with EL2.

Later, another dominant level was discovered in p-type material[189,211,212] at $E_v + 0.5$ eV. Because its concentration is equal to that of EL2 (detected by its level at $E_c - 0.82$ eV), it can be unambiguously ascribed to EL2,[213,214] which therefore appears as a double donor.

The extrinsic absorption spectrum observed in undoped semi-insulating or n-type doped materials,[215] extending from 0.8 eV to the conduction band, must be attributed to EL2 because it reproduces very well the electron photoionization cross section. This is confirmed by the fact that the spectrum exhibits the quenching behavior which is the fingerprint of EL2.

From all this information, it is possible to draw the configuration coordinate diagram of Fig. 10. Attempts have been made to justify the existence of luminescence bands observed by photoluminescence[216,217] and cathodoluminescence[218] in the range 0.62–0.68 eV by using similar configuration coordinate diagrams. It has been suggested that this large luminescence band is in fact due to a combination in variable proportions of two wide bands centered at 0.64 and 0.68 eV.[219–221] These bands are attributed to the presence of EL2 since the 0.63–0.65 eV band presents the same thermal behavior as EL2 under thermal treatment[222] and the kinetics of the luminescence "fatigue" under 1.1 eV photoexcitation is identical to that of the stable to metastable transformation of the defect.[217,223] It has been proposed that this band corresponds to a transition between the valence band and the midgap EL2 level,[222] which is what one should expect from the configuration coordinate diagram of Fig. 10. The reason the band contains a rich structure[219,223] is that the recombination involves shallow acceptor levels as intermediary steps, as revealed by the oscillatory behavior of photoluminescence excitation above the band gap. However, a general agreement has not yet been reached on this identification[224,225] and the possibility that this luminescence involves a recombination between the double acceptor (EL2) and the double donor Ga_{As} should be investigated (see below).

As to the 0.68-eV band, the temperature dependence of its width, shape, and position has been studied in detail.[221] The results show that this dependence can be accounted for by a Huang–Rhys factor $S = 5.5 \pm 0.5$ with a phonon of energy 20 meV, equal to that derived from DLTS and optical DLTS for the transition between the midgap EL2 level and the conduction band. The proof that the 0.68 eV is a recombination involving this transition is given by the fact that the photoluminescence intensity varies with temperature as the inverse of the electron capture cross section, as expected when the nonradiative multiphonon capture enters in competition with the radiative transition.

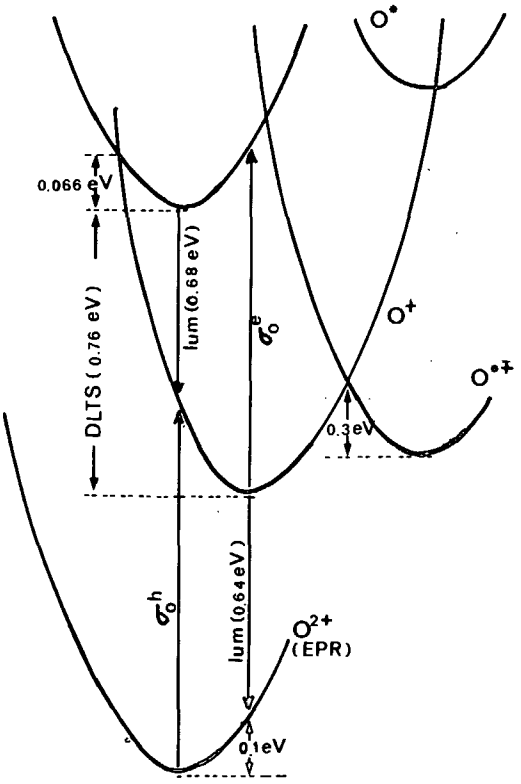

FIG. 10. Configuration coordinate diagram of the EL2 defect for both the stable (O) and metastable (O*) configurations.

C. Thermodynamical characteristics

The correlation between the concentration of EL2 and the crystal stoichiometry has been clearly demonstrated by controlling the growth conditions in bulk as well as in epitaxial materials. The EL2 concentration increases with the As/Ga ratio,[128,129,226–231] strongly suggesting that it is of intrinsic nature and related to a Ga vacancy or an As interstitial or antisite.

Actually, when one compares the stoichiometry dependence of the Ga antisite[127] with that of EL2, one finds a similar but opposite behavior: its concentration decreases with increasing As/Ga ratio. Nevertheless, the total concentrations of these two defects are rather close, which suggests that they should be present together in As as well as in Ga-rich materials and shed a new light on the mechanism for the electrical compensation in semi-insulating materials, as we shall see below.

D. The metastable state

The transition from the stable to the metastable state can only be optically induced. This transition can be monitored by capacitance technique, optical absorption, EPR, etc., as a quenching, i.e., as a disappearance of all properties associated with the EL2 defect in the stable configuration. The cross section σ^* corresponding to the photoinduced transition is centered near 1.15 eV (Ref. 181), and this transition is visible in the optical absorption spectrum. The corresponding absorption band can be obtained as the difference between the electron photoionization spectrum and the EL2 associated optical spectrum properly normalized.[232] This absorption band displays a fine structure interpreted as phonon replica (energy 11 meV) of the zero phonon line lying at 1.04 eV.[232] Actually, it now seems that the zero phonon line itself exhibits a complex structure.[233] The band corresponds to an intracenter transition since this absorption can also take place in a space-charge region. The photocapacitance technique demonstrates[180,181] that the transition conserves the defect charge. This new state is metastable since it has the same charge state as the stable state and is only stable at low temperature. The stable state is regenerated[181,234] by a thermal annealing at ~ 140 K. The kinetics of this regeneration r has been determined. It is thermally activated $[r(s^{-1}) = 2\times 10^{-4} \exp(-0.3\ \text{eV}/kT)]$ and enhanced in the presence of electrons by a Auger like process, i.e., by a factor proportional to the electron concentration.[234] Recently, it has been observed that regeneration can also be induced optically in the 70–140 K range[235–238]; its spectral dependence (centered at 0.8 eV for a 90 K regeneration) is temperature dependent.[239]

E. The identification of EL2

When it appeared that the EPR signal associated with the As antisite exhibits the same photoionization and photoquenching behavior as that of EL2[190,240] it was clear that As_{Ga} is involved in the EL2 configuration and various models were proposed. Among the most popular atomic configurations proposed were (i) the isolated As_{Ga}, because the intracenter transition at 1.04 eV indicates a T_d symmetry for this defect[191], and (ii) the $As_{Ga} + V_{As}$ complex[194,241] which has been predicted to have an EL2-like metastable behavior. The isolated antisite model was first (momentarily) abandoned when it has been demonstrated that the uniaxial stress experiment performed on the 1.04-eV line could perhaps be lower than T_d (Ref. 242) and because it was difficult to imagine the formation of another configuration by such a 1 eV energy for such an isolated substitutional impurity. Vacancy-related defects are ruled out immediately by PA which shows (see Sec. IV) that vacancy defects anneal at a temperature (450 °C) well below the temperature at which EL2 is still stable (950 °C). The $As_{Ga} + V_{As}$ complex, which is produced by electron iradiation (see Sec. III), has a behavior under photoexcitation different from the EL2 one.

A significant step towards EL2 identification was reached with the observation[6,198] that (i) the As_{Ga} EPR spectrum is no longer photoquenchable in a material annealed at 850 °C and quenched to room temperature, and (ii) the spectrum recovers its photosensitivity after an additional heating around 120 °C. It was therefore deduced that EL2 is a complex involving As_{Ga} and an entity X which dissociate into the isolated defects As_{Ga} and X by high-temperature treatment followed by a quench and regenerate by subsequent low-temperature treatment. Because a substitutional atom like As_{Ga} cannot migrate at this low temperature, the regeneration must be due to the migration of X which should then be an interstitial atom. Because As_i migrates in the same temperature range as does X (changes in the atomic configuration of EL2 under uniaxial stress are also observed[243] in this temperature range), it was concluded that $X = As_i$. Recognizing that the EPR spectrum of the EL2 complex cannot be distinguished from that of the isolated As_{Ga} and that the spectrum disappears when EL2 is in its metastable state allowed one to deduce further that the EL2 stable state corresponds to As_{Ga} with As_i in second-neighbor position while, in the metastable state, As_i comes closer to As_{Ga}.[244] The mechanism by which the stable to metastable transformation occurs was suggested to be of Coulombic nature through the internal transfer of an electron from $As_i^{(0/+)}$ to As_{Ga}^0 by the 1.1-eV excitation.[244]

Recently, this model for the stable state has been directly verified by ODENDOR[199,203] which allowed the superhyperfine structure of the defect to be obtained. From this it was deduced that As_i is in a singly positive charge state[199] and located at a [111] tetrahedral site (see Fig. 11). Most of the characteristics of the defect can now be understood on simple theoretical grounds.[245–248] The atomic configuration of the metastable state, which we believe to correspond to an As_{Ga} with an As_i close by, has been derived using theoretical considerations and the corresponding electronic structure has been calculated.[205]

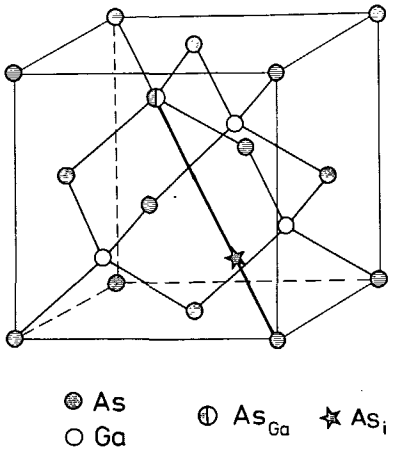

FIG. 11. Atomic configuration of the EL2 defect.

The possibility that the metastable state is a close As_{Ga}-As_i pair was first analyzed by Baraff and Schlüter[248]; unfortunately, they did not include the effect of lattice reorganization although, as suggested in the case of silicon,[249] split-interstitial configurations might be energetically favorable in agreement with theoretical calculations[250,251] that suggest the existence of flat energy surfaces for the migration of self-interstitials. Using this argument and the fact that the coordination of elemental arsenic in the crystalline and amorphous forms is trivalent, one concludes that a quite plausible model for the close pair is the one depicted schematically in Fig. 12. In this model the two central atoms forming the split-interstitial pair are trivalently bonded while the four other atoms retain their normal tetravalent coordination. This split-interstitial configuration should be even more stable in this case than in the silicon in view of the preference of the As atom to form trivalent bonds. A similar conclusion can be obtained from direct thermodynamic arguments. It is known that the cohesive energy per atom in crystalline As is of the order of 3 eV, the same as in GaAs where the nearest-neighbors' distance is also comparable. Knowing that the formation energy of an interstitial atom (i.e., its energy relative to its value at the normal lattice position) is of the order of 4 eV, one is led to conclude that the split-interstitial would be more stable than the separated pair by an amount of the same order of magnitude, i.e., ~4 eV.[251–253] This is not strictly true since such estimate of the split interstitial energy does not include the elastic energy corresponding to lattice deformation around the split interstitial pair. However, angular force constants being weak in

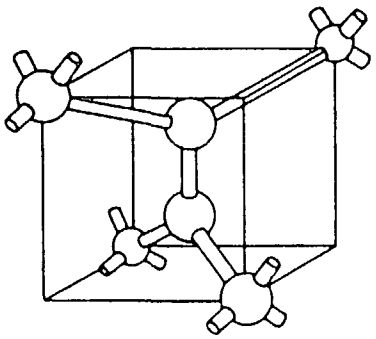

FIG. 12. Schematic representation of the split interstitial configuration.

GaAs, such an energy will be smaller than 4 eV, therefore we expect the split-interstitial pair to be more stable than the separated pair.

The electronic structure of such a split-interstitial configuration can be derived. Let us first recall the essential nature of the band structure in trivalent arsenic using a tight-binding molecular description. As there are three equivalent bonds per atom, we consider on each As atom three equivalent p orbitals pointing approximately towards the nearest neighbors. Coupling between these p orbitals within each bond leads to bonding σ states and antibonding σ^* states, the s state being practically of atomic nature. Inclusion of further interactions broadens the σ and σ^* molecular states into bands and allows some mixing between s and p states. The correspondence between the molecular picture and the true bands is indicated in Fig. 13(a). We can now apply the same description to our split interstitial configuration since the interbond angles have values close to the ones they have in crystalline As. In a similar molecular picture, bond formation will take place between the p orbitals of the two split-interstitial atoms and the sp^3 orbitals of the four As neighbors, resulting in one p-p bond and four p-sp^3 bonds. On the whole, as shown on Fig. 13(b), there will be five σ bonding states and five σ^* antibonding states with two s-like remaining atomic states. As it is expected that the σ-σ^* splitting is larger than the GaAs gap, the resulting situation should be the one depicted in Fig. 13(b). A full calculation of the electronic structure[205] provides essentially the same result. It does not lead to a gap state; this means that the charge state of the defect is determined since there are 2 electrons per bonding state and 2 per s state, i.e., a total of 14 electrons. As a neutral complex would contain 15 electrons (5 on the sp^3 orbitals and 5 per interstitial As atom), the split interstitial configuration just described can only correspond to a 1 + charge state. Thus, the proposed model for the metastable state has no deep-level gap state as experimentally observed. This configuration exists only in a singly positive charge state which precisely corresponds to the quenchable charge state of the stable configuration[245] and agrees with the observation that the charge state of the defect is conserved in the transition.

A search for such a configuration is now being attempted through the detection of the associated localized vibrational modes. However, the preliminary results obtained[253] seem now to indicate that the detected modes are related to interstitial oxygen.[254]

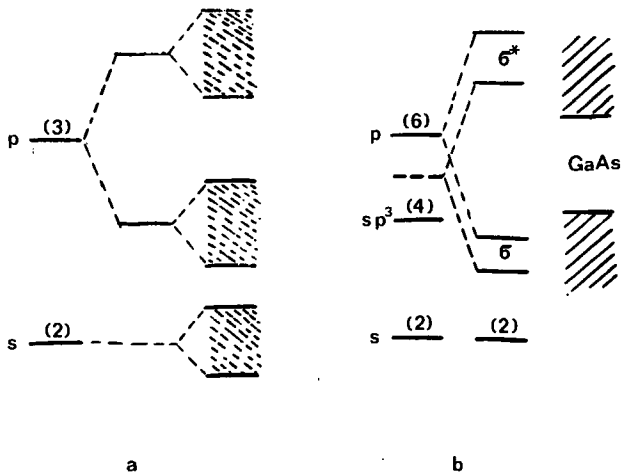

FIG. 13. Band formation in trigonal As (a) and proposed level structure (b) for the split interstitial in relation to the bulk band structure of GaAs.

F. Final remarks

Although in principle a spectroscopic technique, such as ODENDOR in this case, provides unambiguously the atomic configuration of a defect, through the distribution of the components of the wave function on the different atomic sites which surround it, the above identification is apparently not yet fully accepted and new models are still proposed. In particular, recent theoretical results on the isolated As_{Ga} which predicted a metastability in the neutral charge state have led independently two groups[255,256] to suggest that As_{Ga} is the EL2 defect. However, the rich experimental information available for the EL2 defect allows one to test the validity of the different models in detail.

Let us first consider the data obtained on the point symmetry and thermal stability of EL2. The isolated As_{Ga} model predicts for the stable configuration (in both the 0 and + charge states) a T_d symmetry[67,255,256] while the As_{Ga}-As_i^- model predicts for the same charge states a lower symmetry (C_{3v}). This symmetry has been tested by three different techniques: ENDOR, optical absorption, and DLTS under uniaxial stress. The ENDOR technique (which probes the + charge state) shows in semi-insulating GaAs, grown by the LEC method, according to Meyer *et al.*,[199] only one type of As_{Ga}-related defect having a C_{3v} symmetry; in addition, these authors demonstrate that such symmetry is due to the presence of an additional As atom in a (111) direction. In optical absorption, the zero-phonon line attributed to an internal transition of EL2 in the 0 charge state and was first claimed to be of T_d symmetry[191]; however, this result was questioned by Figielski and Wosinski[257] who pointed out an inconsistancy in the interpretation of the data and who proposed an alternative one based on a lower symmetry (C_{2v}). As to DLTS, it shows that the defect can reorient under uniaxial stress for temperatures higher than 150 °C since a preferential population which is metastable can be retained when the sample is cooled to room temperature under stress[243]; from further low-temperature stress results Levison and Kafalas[243] deduced a C_{3v} symmetry from the anisotropy of the quenching transients.

The thermal stability of the defect is also a good test to distinguish between an isolated substitutional defect (As_{Ga}) and a complex involving this defect and an interstitial atom. Indeed, for isolated As_{Ga} we expect a high thermal stability, similar to the one observed for substitutional impurities during diffusion, while for the complex we expect the dissociation to occur at a considerably lower temperature. There are experimental evidences that a thermal treatment at a temperature as low as ~200 °C induces a transformation of the defect configuration: they are the DLTS measurements of Levinson and Kafalas mentioned above, earlier DLTS and

EPR observations already discussed,[198] and recent results of Mochizuki and Ikoma.[258] These last authors have studied the effect of reactive ion etching on the EL2 defect; they observed that the etching process strongly decreases the EL2 concentration in the surface region and that a subsequent anneal at 300 °C leads to a restoration of the initial concentration. These observations can be understood if the defect contains a mobile component such as As_i of the As_{Ga}-As_i model. This is not in contradiction with the apparent stability of the defect under high-temperature annealings: the complex is separated at this temperature but reforms during cooling.

Thus these specific properties ruled out the possibility that the isolated As_{Ga} can be the EL2 defect.

The As_{Ga}-As_i model, in spite of its success in explaining the atomic configuration of EL2, has raised objections concerning (i) the stability of the complex: why is As_i stable in a second-neighbor interstitial position, and (ii) the role of the defect in the electrical compensation, since the total charge of the defect is positive, due to the positively charge state of As_i. However, these objections can be lifted by the following argument. The As antisite involved in EL2 is paired with the Ga antisite.[259] The negatively charged double acceptor Ga_{As} stabilizes As_i by Coulomb attraction. As to the compensation it occurs primarily through the neutralization of the double donor As_{Ga} by the double acceptor Ga_{As}.

Actually, the presence of Ga antisites in stoichiometric materials should not be a surprise; as already mentioned the concentrations of Ga_{As} and As_{Ga} vary with stoichiometry in an opposite way but these variations are small. If one extrapolates these dependencies, from the As- and Ga-rich regions, to the stoichiometric region in which the material becomes semi-insulating, one finds that the concentrations of both antisites are similar, in the range 10^{15}–10^{16} cm^{-3}, a value in agreement with the above measurements. Thus Ga_{As} is present in As-rich materials and As_{Ga} in Ga-rich materials. Additional experimental evidences have been given before for Ga_{As} in an As-rich material by a thermal stimulated current technique[260] and recently by IR absorption after we move the Fermi level by optical quenching of EL2. It is then natural from a thermodynamic point of view to think that, since both As_{Ga} and Ga_{As} are in comparable concentrations in a stoichiometric material, they should be paired because the formation energy for such a pair is smaller than the formation energies of the isolated entities.[261] In fact, preliminary time-resolved photoluminescence[262] clearly points out that the EL2 related donor-acceptor recombination occurs *via* pairs at fixed distance. Moreover, the high electron mobilities ($\sim 5\times10^3$ V/cm^{-2} s) measured in this material do exclude a statistical distribution of the arsenic antisite donors and gallium antisite acceptors, but, again, can be well understood if the antisites are paired.

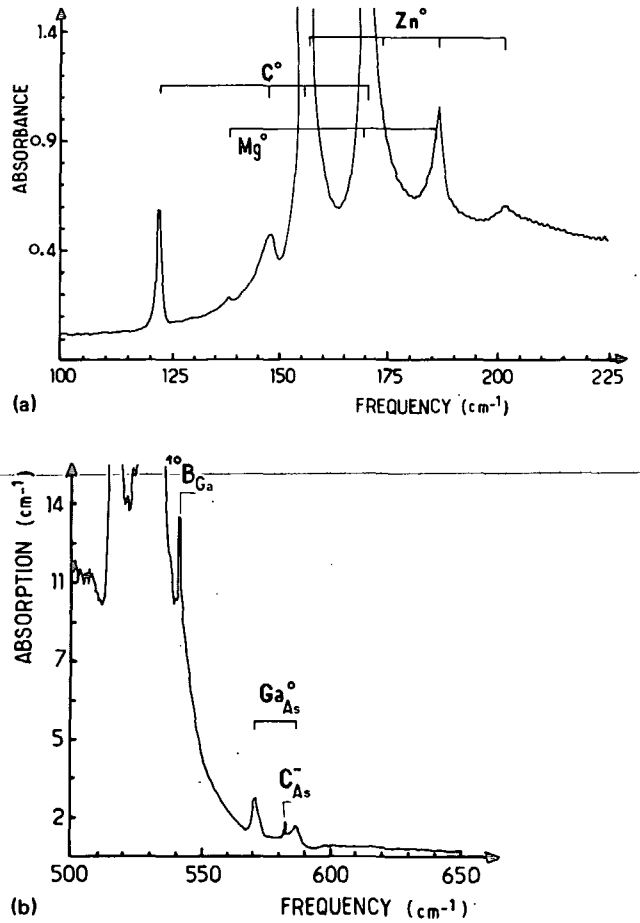

FIG. 14. IR absorption spectra of the native acceptors neutralized by the photoquenching of EL2 (a) and of the intrinsic double acceptor, together with the LVM spectrum of C^{-}_{As} (b).

G. The mechanism for the compensation

The current model for the compensation of the free carrier in stoichiometric semi-insulating material is based on the interaction between the deep donor EL2 and the residual shallow donor and acceptor impurities. The concentrations of the donor and acceptor impurities, N_D and N_A, are such that N_A-N_D compensate, at least partially, the EL2 concentration N_{EL2} so that the Fermi level lies in the vicinity of the EL2 midgap level E_{EL2}. In fact, this picture is far from being satisfying because $N_A \sim 10^{15}$ cm^{-3} and $N_{EL2} \sim 10^{16}$ cm^{-3} while in many cases the Fermi level lies well below E_{EL2}. This model requires a revision to take into account the existence of the double acceptor in a concentration comparable to EL2. In this new model the double acceptors compensate the double donors (EL2) and the degree of compensation is only slightly modified by N_A-N_D (see Fig. 15). This model takes into account the fact that the midgap EL2 level corresponds to a $+/2+$ charge state transition and not to a $0/+$ transition as previously assumed. It is able to reproduce quantitatively the electrical properties of the material as well as their variations with the stoichiometry: this has been already demonstrated by Figielski.[263] As sketched in Fig. 15 it reproduces the carrier concentration dependence with the melt stoichiometry.

VI. POINT DEFECTS, DISLOCATIONS, AND MATERIAL HOMOGENEITY

A. Isolated defects

The picture we deduce from the electronic properties described in Sec. IV is the following: the material contains a

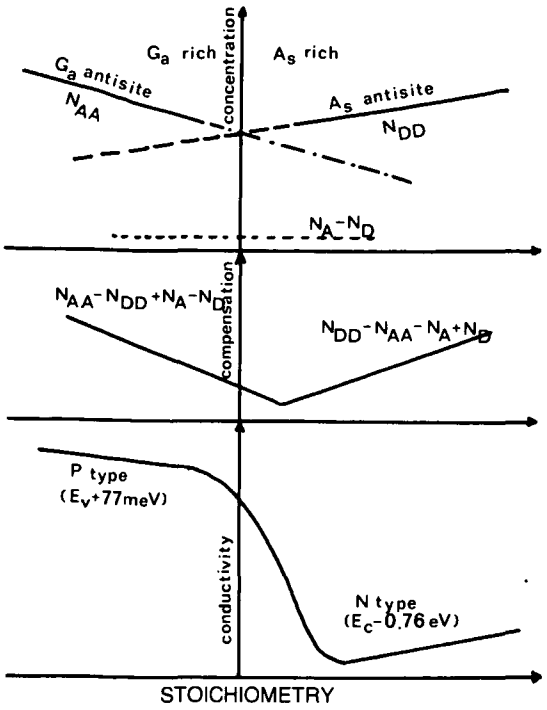

FIG. 15. Schematic representation of the variation of the antisite concentrations, of the residual free-carrier concentration (compensation) and of the conductivity vs melt stoichiometry.

series of defects whose nature and concentration depend on the way the material is grown. Apparently, EL2 is the only defect common to all materials, provided they are As rich. These defects compensate, partially or totally, the residual acceptor impurities and the doping impurity. Their total concentration is in the range 10^{16}–10^{17} cm^{-3} in bulk materials (LEC, HB) and ~ 100 times lower in epitaxial materials. All these defects, except EL2, anneal out by thermal treatment at 850 °C.

A comparison of the electronic characteristics of these native defects with those of simple intrinsic defects described in Sec. III shows that none of them are simple intrinsic defects with the exception of the antisites Ga_{As} and As_{Ga} under the form of EL2. This implies that all other native defects are complexes involving intrinsic defects in interaction with themselves or with impurities. Nothing more can be said on their nature since they have not really been studied. In addition, As interstitials should be present in As-rich materials. The existence of the complex EL2, an As_i bound in the vicinity of an As_{Ga} with a rather low binding energy (0.6 eV), suggests that the material contains sources of As_i. The defect EL2 is only apparently stable at high temperature where one expects the complex $As_{Ga} + As_i$ to be dissociated and only As_{Ga} and Ga_{As} to remain stable.

It therefore appears that the way a material is cooled down should be an important factor governing the nature and concentration of the defects it contains at room temperature or below and, consequently, its electrical properties. This is illustrated by the effect of "slow" and "fast" cooling which reversibly changes the electrical properties of LEC materials from semiconducting to semi-insulating.[264] As demonstrated by Look *et al.*,[265] this effect cannot be accounted for by a change in the balance between donor and acceptor impurities. In our view it is related to a change in the nature of the defects, the balance between donor- and acceptor-type defects being governed by the characteristic time for As_i trapping on these defects relative to the rate of cooling. It is probably this reason which also explains the thermal conversion induced by modifications in post-solidification treatment observed in Ref. 266.

B. Dislocation-associated defects

The other techniques of detection, i.e., DTA and PA, which are not based on the electronic properties of the defects, provide a completely different picture. They indicate that a bulk material contains 10^{17}–10^{18} cm^{-3} vacancy-related defects. In *n*-type doped HB materials DTA shows that these defects anneal around 450 °C. The activation energy of the annealing (2.2 eV) is equal, within the experimental accuracy, to the activation energy associated with the maximum strain rate measured in creep tests[267] in similarly doped materials (according to Ref. 268, such activation energy corresponds to a stress of ~ 2 kg mm^{-2}). This suggests that the defects detected by DTA are associated with dislocations and that they anneal when the dislocations become mobile since no DTA signal is observed in LEC materials where the dislocations cannot move. However, it is possible that this defect concentration is overestimated because of (i) an underestimation of the positron trapping rate and (ii) because mobile dislocations generate defects which are also detected by DTA. Indeed it has been shown that stress induced deformation introduces defects[115,116,269] although the observed introduction of EL2[116] could result from a change of the Fermi level. The fact that dislocations are decorated with defects is well known. The regions surrounding dislocation networks show a strong variation of resistivity and luminescence intensity.[270–274] X-ray diffraction has shown that the regions surrounding dislocations have a higher As concentration than the bulk material.[275] Stirland was the first to report the existence of dislocation-associated precipitates[276] in Ga-rich material, which were subsequently detected in undoped materials.[277] Moreover, large As precipitates (500 Å diameter) have been detected by high-resolution diffraction.[278]

On the other hand, PA indicates the presence of additional vacancy related defects which anneal at the same temperature. It is thus natural to deduce that, when dislocations move, the As precipitates dissociate and liberate As_i which then recombine with these vacancy defects. These As_i, having a small migration energy (see Sec. III), can migrate long distances and interact with other isolated defect, giving rise to complexes such as the one detected by EPR (see Sec. IV). Because the velocity of dislocations is carrier concentration dependent, this annealing process should depend on the nature and concentration of the doping impurities. It should also be shifted to higher temperatures when the density of dislocations is high since their interaction prevents their mobility from taking place (for a review on dislocations and their interaction with point defects, see Ref. 279).

The fact that dislocations are decorated with a large concentration of defects is a strong indication that they act as

gettering centers for mobile defects. This gettering has indeed been directly observed by cathodoluminescence.[280] Thus vacancy-related defects, as well as the interstitials present during the growth, cluster in the strain fields of the dislocations when the material is cooled down.

This gettering phenomenon should also occur for the damage produced by ion implantation. One then expects that cylindrical regions around dislocations, with a radius R depending on the temperature and annealing time, will be free of defects and that, consequently, an annealed implanted layer will have a free-carrier concentration in these regions larger than in the rest of the layer. Indeed, an implanted layer, once annealed, is partially compensated by the remaining defects; DLTS shows that approximately 10% of the free carriers are compensated by defects in an implanted layer after a 850 °C anneal under a Si_3N_4 cap. The profile of these remaining defects around the dislocations should produce a decrease of the free-carrier concentration as the distance from the center of the dislocation increases. Such variation in the sheet carrier concentration as a function of the distance between a micro Hall chip and a dislocation pit has been indeed observed.[281] It provides a radius $R = 50\,\mu$m in the case of a 5×10^{12} cm^{-2}, 60-keV Si implantation followed by an 800 °C, 20-min. (Si_4N_4 cap) annealing, which correlates directly with the variation of the threshold voltage of FETs as a function of their distance from dislocations.[281,282]

High-resolution scanning photoluminescence allows a qualitative observation of the defect and impurity distribution around the dislocations. In LEC materials the dislocations appear as dark spots (of radius $\sim1\,\mu$m) surrounded by regions of high luminescence intensity, typically 10 μm.[283] This demonstrates that they contain a high defect concentration located within a 1 μm radius from the center, while the surrounding area is depleted from nonradiative centers, i.e., from defects. Through the photon energy dependence of the luminescence intensity showing band-to-band recombination, which is related to donor- or acceptor-to-band transitions, it is possible to deduce that the concentration of isolated donor or acceptor impurities increases with the distance from the dislocation.[284,285] Since this variation cannot be due to the presence of nonradiative centers (because their concentration also increases with the distance), this observation implies that the acceptor impurities are also depleted around dislocations, i.e., they are also gettered. This result is confirmed by the fact that the luminescence intensity can be considerably higher in the region surrounding the dislocations than far from them where nonradiative defect centers are present.[286]

From an evaluation of the radius of the region which contains the defects ($\sim1\,\mu$m) it is possible to evaluate the defect density in this region. Using DTA data relative to HB materials containing $\sim5\times10^3$ EPD cm^{-2}, which indicate the annealing of $\sim5\times10^{17}$ cm^{-3} defects, one gets a defect density of $\sim3\times10^{21}$ cm^{-3}. This means that the region around a dislocation is indeed heavily disordered.

C. The source of interstitials

Obviously, the As clusters attached to dislocations are sources of As_i. This is demonstrated by the disappearance at 450 °C of vacancy-related defects, detected by PA, and of isolated V_{As}, detected by EPR, in electron-irradiated materials. However, there may be other As clusters present, independent of dislocations, since for thermal treatments above 450 °C a source of As_i still exists. This is in agreement with the observation of Barett *et al.*,[287] who have detected isolated As-rich clusters in dislocation-free areas using energy dispersive x-ray analysis.

The smallest isolated cluster in the As antisite which has not been detected as a native defect. However, it is present in the form of EL2, a cluster of six As atoms. This defect is practically uniformly distributed in the material, its concentration being determined by the stoichiometry. The optical absorption at 1.1 μm, which is widely used to draw contour maps of EL2 concentration, provides fourfold symmetric patterns having a W shape across a wafer.[288–290] The reason is that this technique only probes that population of the EL2 defects which has the As_{Ga} in the neutral charge state; the W shape reflects the fluctuations of the Fermi level which is determined, in semi-insulating materials, by the compensation. As demonstrated by Spaeth,[204] when both charge states of EL2 are taken into account, its distribution is uniform. The same reasoning applies also to the luminescence techniques.[291]

There may be other As antisite related defects, such as As_{Ga} pairs, which eventually could also trap one or several As_i leading to larger As clusters. In its metastable form, EL2 corresponds to the smallest arsenic aggregate (see Sec. V) with two trivalently bonded central atoms. Larger As clusters will also probably be in the amorphous phase since As bonding is trivalent. Ponce *et al.*[292,293] suggest in fact that the microdefects they observe by high-resolution transmission microscopy inside dislocation cells are indeed amorphous precipitates. Such amorphous aggregates probably will not be detected by electronic techniques since they should not give rise to localized levels inside the gap of the material. This can be easily demonstrated by following the same line of reasoning as that used to derive the electronic structure of the metastable state of EL2 (see Sec. V). Heat treatment should lead to the dissociation of such clusters. It is this way we understand the eventual increase of the EL2 concentration after 800–1100 °C annealing[294] which transforms large clusters into smaller ones.

Another possible source (or sink) of As is the surface and the contact atmosphere. As loss is known to occur on heating above $\sim$650 °C when the surface is not protected. If the surface is a source, this should depend strongly on the way the surface is encapsulated. In bulk materials, heat treated in conditions favorable to As loss, acceptor defects are introduced[295–297] which should be Ga antisites since the surface exhibits[298] a luminescence band at 1.44 eV (see Sec. III). Conversely, heat treatment under an Si_3N_4 encapsulant, which increases the As/Ga ratio,[299] could introduce As antisites, i.e., EL2. This has been observed apparently in MBE layers which do not initially contain EL2. However, in bulk materials no such increase has been observed. In fact, there are conflicting results. The EL2 concentration has been reported to increase[22] or to decrease.[300] This apparent discrepancy is probably due to the influence of the capping

material, its stoichiometry, and of the ambient environment (hydrogen, vacuum, etc.) in which the annealing is performed.[22] Actually, the situation is probably more complicated since both donor and acceptor defects are introduced near the surface with concentrations depending strongly on the As pressure.[301] From the profile of the donor, Chiang and Pearson[301] deduced an activation energy of 0.4 eV associated with the out-diffusion of this defect, a value close to the one known for As_i migration (see Sec. III).

D. On material homogeneity

The defects we have described, because of their nature and distribution, give rise, as a result, to a highly inhomogeneous material. This material can be described as a semiconducting medium containing uniformly distributed impurities (some of which are introduced intentionally, such as the doping impurities, and others not such as the residual shallow impurities) and point defects which compensate partially or totally the shallow impurities. Imbedded in the material are line defects composed of dislocations decorated by heavily disordered regions and surrounded by larger regions in which point defects and impurities concentrations vary and As clusters, of various sizes, which are probably amorphous.

Some of the As clusters are located on the dislocation lines but is not clear if there is also an inhomogeneous distribution of these clusters induced by the dislocations around them. Indeed, the observation of an apparent large concentration of EL2 in dislocated regions[302,303] can be ascribed to the change in Fermi-level position in these regions.

Both clusters and dislocation associated disordered regions cannot be detected by the electronic techniques described in Sec. II because they give rise to insulating regions which introduce potential fluctuations. The transition between these regions and the rest of the material is insured by band bending. They leave unchanged the carrier mobility because their size is larger than the mean free path. They cannot be seen by luminescence since the band curvature separates spatially electrons and holes preventing their recombination. They are not detected by DLTS because the associated localized levels, if any, are too deep (below the middle of the gap) to emit carriers in the temperature range where this technique is usually applicable. However, such potential fluctuations can be seen by probing at the same time charge states of several defects having energy levels at different positions in the forbidden gap.[304] In addition, these fluctuations give rise to a long-range disorder similar to the one existing in amorphous materials. They change the carrier transport coefficients as well as their temperature and frequency dependence.[305] The results of ac and dc conductivity measurements[306–310] indeed confirm the existence of such potential fluctuations and provide a way to evaluate them. Dielectric spectroscopy,[311] because it is capable of looking in detail at "horizontal" transitions (i.e., between localized states) in semi-insulation materials, should give additional information.

Thus one way of improving material homogeneity is to perform thermal treatment long enough to allow the As precipitates to dissolve and to decrease the defect density along dislocations.[312] However, in case of ion implantation, the dislocations will getter the defects produced in their neighborhood.

VII. CONCLUSION

GaAs materials contain several point defects which are complexes of simple intrinsic defects or of intrinsic defects with impurities. The only simple intrinsic defects present as native defects are the As and Ga antisites both detected in As- and Ga-rich materials, respectively. However, bulk materials are highly inhomogeneous because they contain (i) dislocations which getter point defects as well as impurities, resulting in a heavily disordered core region surrounded by a larger region free of defects and impurities and (ii) small As clusters such as EL2 and larger ones. These As clusters, as well as the ones decorating the dislocations, are sources of As interstitials which play a role during thermal treatment. Because of their gettering ability, the dislocations prevent the material from becoming homogeneous even after ion implantation. However, this homogeneity can be improved by thermal treatment which anneals, at least partially, the defects attached to them and dissociates the As clusters.

ACKNOWLEDGMENT

This work has been supported by a Thomson-CSF grant.

[1]G. M. Martin, J. P. Farges, G. Jacob, J. P. Hallais, and G. Poiblaud, J. Appl. Phys. **51**, 2840 (1980).
[2]G. Stillman, B. Lee, and S. Bose (unpublished).
[3]P. M. Mooney (unpublished).
[4]M. Lannoo and J. C. Bourgoin, *Point Defects in Semiconductors, I—Theoretical Aspects* (Springer, Berlin, 1981).
[5]J. C. Bourgoin and M. Lannoo, *Point Defects in Semiconductors, II—Experimental Aspects* (Springer, Berlin, 1983).
[6]H. J. von Bardeleben, D. Stievenard, J. C. Bourgoin, and A. Huber, Appl. Phys. Lett. **47**, 970 (1985).
[7]H. L. Lim, H. J. von Bardeleben, and J. C. Bourgoin, J. Appl. Phys. **62**, 2738 (1987).
[8]C. M. Wolfe, G. E. Stillman, D. L. Spears, and F. V. Williams, J. Appl. Phys. **44**, 732 (1973).
[9]G. B. Stringfellow, J. Appl. Phys. **53**, 5345 (1982).
[10]D. V. Lang, J. Appl. Phys. **45**, 3023 (1974).
[11]D. Stievenard and D. Vuillaume, J. Appl. Phys. **60**, 973 (1986).
[12]D. Pons, Appl. Phys. Lett. **37**, 413 (1980).
[13]F. Poulin and J. C. Bourgoin, Phys. Rev. B **26**, 6788 (1982).
[14]D. Pons, J. Appl. Phys. **55**, 3644 (1984).
[15]D. Stievenard, J. C. Bourgoin, and M. Lannoo, J. Appl. Phys. **55**, 1477 (1984).
[16]D. Stievenard and J. C. Bourgoin, J. Appl. Phys. **59**, 808 (1986).
[17]A. Chantre, G. Vincent, and D. Bois, Phys. Rev. B **15**, 5335 (1981).
[18]D. Stievenard, M. Lannoo, and J. C. Bourgoin, Solid State Electron. **28**, 485 (1985).
[19]M. O. Watanabe, A. Tanaka, T. Udagawa, T. Nakanisi, and Y. Zohta, Jpn. J. Appl. Phys. **22**, 923 (1983).
[20]F. Hasegawa, M. Tomakane, N. Yamamoto, and T. Nakanisi, in *Semi-Insulating III–V Materials*, edited by H. Kukimoto and S. Miyazawa (Ohmsha, North-Holland, Amsterdam, 1986), p. 471.
[21]J. Lagowski, D. G. Lin, T. Aoyama, and H. C. Gatos, Appl. Phys. Lett. **44**, 336 (1984).

[22]F. Hasegawa, M. Yamamoto, and Y. Nannichi, Appl. Phys. Lett. **45**, 461 (1984).
[23]S. Makram-Ebeid, Appl. Phys. Lett. **37**, 464 (1980).
[24]G. M. Martin and S. Makram-Ebeid, in *Deep Centers in Semiconductors*, edited by S. T. Pantelides (Gordon & Breach, New York, 1986), Chap. 6.
[25]J. Lagowski, H. C. Gatos, J. M. Parsey, K. Wada, M. Kaminska, and W. Walukiewicz, Appl. Phys. Lett. **40**, 342 (1982).
[26]A. Broniatowski, A. Blosse, P. C. Srivastava, and J. C. Bourgoin, J. Appl. Phys. **54**, 2907 (1983).
[27]H. Zhang, Y. Aoyagi, S. Iwai, and S. Namba, Appl. Phys. Lett. **50**, 341 (1987).
[28]D. L. Loose, J. Appl. Phys. **46**, 2204 (1975).
[29]G. Vincent, D. Bois, and P. Pinard, J. Appl. Phys. **46**, 5173 (1975).
[30]D. V. Lang and C. H. Henry, Phys. Rev. Lett. **35**, 1525 (1975).
[31]C. H. Henry and D. V. Lang, Phys. Rev. B **15**, 989 (1977).
[32]D. Pons and S. Makram-Ebeid, J. Phys. (Paris) **40**, 1161 (1979).
[33]D. Pons, A. Mircea, and J. C. Bourgoin, J. Appl. Phys. **51**, 4150 (1980).
[34]D. Stievenard, X. Boddaert, and J. C. Bourgoin, Phys. Rev. B **34**, 4048 (1986).
[35]D. Pons and J. C. Bourgoin, J. Phys. **18**, 3839 (1985).
[36]For a review, see J. C. Bourgoin and J. W. Corbett, Radiat. Eff. **36**, 157 (1978).
[37]J. C. Bourgoin and J. W. Corbett, IEEE Trans. Nucl. Sci. **NS-18**, 11 (1971).
[38]C. E. Barnes, Phys. Rev. B **1**, 4735 (1970).
[39]D. V. Lang and L. C. Kimerling, Phys. Rev. Lett. **35**, 22 (1975).
[40]D. Stievenard and J. C. Bourgoin, Phys. Rev. B **33**, 8410 (1986).
[41]J. C. Bourgoin and J. W. Corbett, Phys. Lett. **38A**, 135 (1972).
[42]Y. Fujiwana, T. Nishino, and Y. Hamakawa, Jpn. J. Appl. Phys. **21**, L727 (1982).
[43]G. P. Peka, L. G. Shepel, and L. Z. Mirets, Sov. Phys. Semicond. **7**, 1439 (1974).
[44]D. C. Reynolds, C. W. Litton, R. J. Almassy, G. L. McGoy, and S. B. Nam, J. Appl. Phys. **51**, 4842 (1980).
[45]H. P. Gislason, Z. G. Wang, and B. Monemar, J. Appl. Phys. **58**, 240 (1985).
[46]For a review, see P. J. Dean, Prog. Cryst. Growth Charact. **5**, 89 (1982).
[47]For a review see J.-M. Spaeth, in *Defects in Semiconductors, Material Science Forum*, edited by H. J. von Bardeleben (Trans Tech, Aedermannsdorf, Switzerland, 1986), Vol. 10–12, p. 505.
[48]W. G. Spitzer and W. Albred, J. Appl. Phys. **39**, 4999 (1968).
[49]For a review, see R. C. Newman, in *Thirteenth International Conference on Defects in Semiconductors*, edited by L. C. Kimerling and J. M. Parsey (The Metallurgical Society of AIME, New York, 1985), p. 87.
[50]H. Lim, H. J. von Bardeleben, and J. C. Bourgoin, Phys. Rev. Lett. **58**, 2315 (1987).
[51]J. C. Bourgoin, H. J. von Bardeleben, and D. Stievenard, Phys. Status Solidi A **102**, 499 (1987).
[52]J. C. Bourgoin, H. J. von Bardeleben, D. Stievenard (unpublished).
[53]M. Stucky, C. Corbel, B. Geffroy, M. Moser and P. Hautojarvi, in *Defects in Semiconductors, Material Science Forum*, edited by H. J. von Bardeleben (Trans Tech, Aedermannsdorf, Switzerland, 1986), Vol. 10–12, p. 265.
[54]G. Dlubek and O. Brümmer, Ann. Phys. **43**, 178 (1986).
[55]A. Bharathi, K. V. Gopinathan, C. S. Sundai, and B. Viswanathan, Pramaña **13**, 625 (1979).
[56]D. P. Kerr, S. Kupca, and B. G. Hogg, Phys. Lett. **88A**, 429 (1982).
[57]A. S. Gupta, S. V. Naidu, R. K. Bhandari, and P. Sen, Phys. Lett. **104A**, 117 (1982).
[58]O. Takai, Y. Hisamatsu, N. Owada, H. Ishimura, K. Hinode, S. Tanigawa, and M. Doyoma, Phys. Lett. **76A**, 157 (1980).
[59]P. Hautojärvi, P. Moser, M. Stucky, C. Corbel, and F. Plazaola, Appl. Phys. Lett. **48**, 809 (1986).
[60]S. Dannefaer, J. Phys. C **15**, 599 (1982).
[61]S. Dannefaer, B. Hogg, and D. Kerr, Phys. Rev. B **30**, 3355 (1984).
[62]G. Dlubek, O. Brümmer, F. Plazaola, and P. Hautojärvi, J. Phys. C **19**, 331 (1986).
[63]S. Dannefaer and D. Kerr, J. Appl. Phys. **60**, 591 (1986).
[64]G. Dlubek, R. Krause, O. Brümmer, and J. Tittes, Appl. Phys. A **41**, 1 (1986).
[65]G. A. Baraff and M. Schlüter, Phys. Rev. B **30**, 1853 (1984).
[66]M. Lannoo, in *Current Issues in Semiconductor Physics*, edited by A. M. Stoneham (Hilger, Bristol, 1986), p. 27.
[67]C. B. Bachelet, M. Schlüter, and G. Baraff, Phys. Rev. B **27**, 2545 (1983).
[68]J. Dow, Mater. Res. Soc. Symp. Proc. **46**, 71 (1985).
[69]J. C. Bourgoin, A. Mauger, and H. J. von Bardeleben, in Proceedings of the Fifth Conference on Semi-Insulating III-V Materials (Malmö, 1988) (to be published); J. C. Bourgoin and A. Mauger, Appl. Phys. Lett. **53**, 749 (1988).
[70]For a review, see D. V. Lang, in *Deep Centers in Semiconductors*, edited by S. T. Pantelides (Gordon & Breach, New York, 1986), p. 489.
[71]T. M. Morgan, Phys. Rev. B **34**, 2664 (1986).
[72]D. Pons, J. Appl. Phys. **55**, 2839 (1984).
[73]F. H. Eisen, Phys. Rev. **135A**, 1394 (1964).
[74]K. Thommen, Phys. Rev. **174**, 938 (1968).
[75]K. Thommen, Radiat. Eff. **2**, 201 (1970).
[76]L. W. Aukerman and R. D. Graft, Phys. Rev. **127**, 1576 (1962).
[77]D. V. Lang, J. Appl. Phys. **45**, 3023 (1974).
[78]D. V. Lang and L. C. Kimerling, Phys. Rev. Lett. **33**, 489 (1974).
[79]D. V. Lang and L. C. Kimerling, Inst. Phys. Conf. Ser. **23**, 589 (1975).
[80]D. V. Lang and L. C. Kimerling, Appl. Phys. Lett. **28**, 234 (1976).
[81]D. Pons, P. M. Mooney, and J. C. Bourgoin, J. Appl. Phys. **51**, 2038 (1980).
[82]D. Pons and J. C. Bourgoin, Phys. Rev. Lett. **47**, 1293 (1981).
[83]D. Pons, Physica B **116**, 388 (1983).
[84]D. Pons, A. Mircea, and J. C. Bourgoin, J. Appl. Phys. **51**, 4150 (1980).
[85]H. J. von Bardeleben, A. Miret, H. Lim, and J. C. Bourgoin, J. Phys. C **20**, 1353 (1987).
[86]S. Loualiche, A. Nouilhat, G. Guillot, A. Laugier, and J. C. Bourgoin, J. Appl. Phys. **53**, 8691 (1982).
[87]R. C. Newman and J. Woodhead, J. Phys. C **17**, 1405 (1984).
[88]M. R. Brozel and R. C. Newman, J. Phys. C **11**, 3135 (1978).
[89]J. Woodhead and R. C. Newman, J. Phys. C **14**, L345 (1981).
[90]H. J. von Bardeleben and J. C. Bourgoin, Phys. Rev. B **33**, 2890 (1986).
[91]R. J. Wagner, J. J. Krebs, G. H. Stauss, and A. M. White, Solid State Commun. **36**, 15 (1980).
[92]H. J. von Bardeleben and J. C. Bourgoin, J. Appl. Phys. **58**, 1041 (1985).
[93]N. K. Goswami, R. C. Newman, and J. E. Whitehouse, Solid State Commun. **40**, 473 (1981).
[94]R. B. Beall, R. C. Newman, J. E. Whitehouse, and J. Woodhead, J. Phys. C **17**, 2653 (1984).
[95]G. D. Watkins, in *Radiation Damage in Semiconductors*, edited by P. Baruch (Dunod, Paris, 1965), p. 97.
[96]H. J. von Bardeleben, J. C. Bourgoin, and A. Miret, Phys. Rev. B **34**, 1360 (1986).
[97]A. A. Rezazadeh and D. W. Palmer, J. Phys. C **18**, 43 (1985).
[98]G. O. Watkins, F. Rong, and W. Barry, Proceedings of the Material Research Society (Boston, 1987) (to be published).
[99]T. A. Kennedy and M. G. Spencer, Phys. Rev. Lett. **57**, 2690 (1986).
[100]M. Lannoo, Phys. Rev. B **36**, 9355 (1987).
[101]P. W. Yu and D. C. Reynolds, J. Appl. Phys. **53**, 1263 (1982).
[102]L. B. Ta, H. M. Hobgood, and R. N. Thomas, Appl. Phys. Lett. **41**, 1091 (1982).
[103]P. W. Yu, W. C. Mitchel, M. G. Mier, S. S. Li, and W. L. Wang, Appl. Phys. Lett. **41**, 532 (1982).
[104]P. W. Yu, Phys. Rev. B **27**, 7779 (1983).
[105]K. R. Elliott, Appl. Phys. Lett. **42**, 274 (1983).
[106]S. G. Bishop, B. V. Shanabrook, and W. J. Moore, J. Appl. Phys. **56**, 1790 (1984).
[107]K. R. Elliott, D. E. Holmes, R. T. Chen, and C. G. Kirkpatrick, Appl. Phys. Lett. **40**, 898 (1982).
[108]P. Filliard, M. Castagne, J. Bonnafé, and M. de Murcia, J. Appl. Phys. **54**, 6767 (1983).
[109]S. R. Morrison, R. C. Newman, and F. Thomson, J. Phys. C **7**, 633 (1974).
[110]M. Mihara, M. Mannoh, K. Shinozaki, S. Naritsuka, and M. Ishii, Jpn. J. Appl. Phys. **25**, L611 (1986).
[111]H. J. von Bardeleben, D. Stiévenard, H. R. Zelsmann, and J. C. Bourgoin, in *Proceedings of the Fifth Conference on Semi-Insulating III-V Materials*, Malmö, 1988 (to be published).
[112]S. Loualiche, G. Guillot, A. Nouilhat, and M. Lannoo, Phys. Rev. B **30**, 5822 (1984).
[113]S. Loualiche, G. Guillot, A. Nouilhat, and M. Lannoo, Solid State Commun. **51**, 509 (1984).
[114]T. Ishida, K. Maeda, and S. Takenchi, Appl. Phys. **21**, 257 (1980).
[115]T. Wosinski, A. Morawski, and T. Figielski, Appl. Phys. A **30**, 233 (1983).
[116]E. R. Weber, H. Ennen, U. Kaufmann, J. Windscheif, J. Schneider, and T. Wosinski, J. Appl. Phys. **53**, 6140 (1982).
[117]P. M. Petroff, R. A. Logan, and A. Savage, Phys. Rev. Lett. **44**, 287

(1980).
[118]K. H. Kuesters, B. C. De Cooman, and C. B. Carter, Philos. Mag. A **53**, 141 (1986).
[119]C. M. H. Driscoll and A. F. W. Willoughby, Inst. Phys. Conf. Ser. **16**, 377 (1973).
[120]G. L. Pearson, H. R. Potts, and V. G. Macres, in *Radiation Damage in Semiconductors*, edited by P. Baruch (Dunod, Paris, 1964), p. 197.
[121]H. R. Potts and G. L. Pearson, J. Appl. Phys. **37**, 2098 (1986).
[122]G. A. Baraff and M. Schlüter, Phys. Rev. Lett. **55**, 1327 (1985).
[123]G. A. Baraff and M. Schlüter, Phys. Rev. B **33**, 7346 (1986).
[124]V. T. Bublik, V. V. Karataev, R. S. Kulagin, M. G. Melerdskii, V. B. Osvenskii, O. G. Stolyarov, and L. P. Kholoduyi, Sov. Phys. Cristallogr. **18**, 218 (1973).
[125]A. F. W. Willoughby, C. M. H. Driscoll, and B. A. Bellamy, J. Mater. Sci. **6**, 1389 (1971).
[126]D. E. Holmes, R. T. Chen, K. R. Elliott, and C. G. Kirkpatrick, Appl. Phys. Lett. **40**, 46 (1982).
[127]J. Lagowski, H. C. Gatos, J. M. Parsey, K. Wada, M. Kaminska, and W. Walukiewicz, Appl. Phys. Lett. **40**, 342 (1982).
[128]M. D. Miller, G. H. Olsen, and M. Ettenberg, Appl. Phys. Lett. **31**, 538 (1977).
[129]P. K. Bhattacharya, J. W. Ku, S. J. T. Owen, V. Aebi, C. B. Cooper, and R. L. Moon, Appl. Phys. Lett. **36**, 304 (1980).
[130]E. E. Wagner, D. E. Mars, G. Hom, and G. B. Stringfellow, J. Appl. Phys. **51**, 5434 (1980).
[131]L. Samuelson, P. Omling, H. Titze, and H. G. Grimmeis, J. Cryst. Growth **55**, 164 (1981).
[132]M. O. Watanabe, A. Tanaka, T. Nakanisi, and Y. Zohta, Jpn. J. Appl. Phys. **20**, L429 (1981).
[133]U. Kaufmann, J. Windscheif, M. Bauemler, J. Schneider, and F. Köhl, in *Semi-Insulating III-V Materials*, edited by D. C. Look and J. Blakemore (Shiva, New York, 1984), p. 246.
[134]A. Ashby, G. G. Roberts, D. J. Ashen, and J. B. Mullin, Solid State Commun. **20**, 61 (1976).
[135]A. Mircea and A. Mitonneau, Appl. Phys. **8**, 15 (1975).
[136]H. Lefevre and M. Schulz, Appl. Phys. **12**, 45 (1977).
[137]D. V. Lang and R. A. Logan, J. Electron. Mater. **4**, 1053 (1975).
[138]D. V. Lang, A. Y. Cho, A. C. Gossard, M. Ilegems, and W. Wiegman, J. Appl. Phys. **47**, 2558 (1976).
[139]K. Sakai and T. Ikoma, Appl. Phys. **5**, 165 (1974).
[140]S. Sheng, D. H. Li, and C. G. Choi, Appl. Phys. Lett. **47**, 1180 (1985).
[141]P. K. Bhattacharya, J. W. Ku, S. J. T. Diven, V. Aeli, C. B. Cooper, and R. L. Woon, Appl. Phys. Lett. **36**, 304 (1980).
[142]Y. Kitagawara, N. Moto, T. Takahashi, and T. Takenaka, Appl. Phys. Lett. **48**, 1664 (1986).
[143]M. O. Watanabe, A. Tanaka, T. Velagawa, T. Nakanisi, and Y. Zehta, Jpn. J. Appl. Phys. **22**, 923 (1983).
[144]P. Blood and A. D. C. Ghassie, Phys. Rev. B **27**, 2548 (1983).
[145]A. Mitonneau, A. Mircea, G. M. Martin, and D. Pons, Rev. Phys. Appl. **14**, 853 (1979).
[146]D. S. Day, J. D. Oberstai, T. J. Drummond, H. Mockoç, A. Y. Cho, and B. G. Streetman, J. Electron. Mater. **10**, 445 (1981).
[147]W. R. Buchwald, N. M. Johnson, and L. P. Trombetta, Appl. Phys. Lett. **50**, 1007 (1987).
[148]A. Humbert, L. Hollan, and D. Boris, J. Appl. Phys. **47**, 4137 (1976).
[149]G. M. Martin, A. Mitonneau, and A. Mircea, Electron. Lett. **13**, 191 (1977).
[150]F. D. Auret, A. W. R. Leitch, and J. S. Vermaak, J. Appl. Phys. **59**, 158 (1986).
[151]A. Mitonneau, G. M. Martin, and A. Mircea, Electron. Lett. **13**, 666 (1977).
[152]A. Mitonneau, A. Mircea, G. M. Martin, and D. Pons, Phys. Rev. B **14**, 3539 (1976).
[153]A. K. Saxena, J. Instrum. Telecom. **26**, 293 (1980).
[154]K. Sakai and T. Ikoma, Appl. Phys. **5**, 165 (1974).
[155]H. Hasegawa and A. Majerfeld, Electron. Lett. **11**, 286 (1975).
[156]F. D. Auret and M. Nel, Appl. Phys. Lett. **48**, 130 (1986).
[157]M. Henini, B. Tuch, and C. J. Paull, Solid State Electron. **29**, 483 (1986).
[158]D. C. Reynolds, C. W. Litton, R. J. Almassy, G. L. McCoy, and S. B. Nam, J. Appl. Phys. **51**, 4842 (1980).
[159]A. Chantre and L. C. Kimerling, in *Defects in Semiconductors, Material Science Forum*, edited by H. J. von Bardeleben (Trans Tech, Aedermannsdorf, Switzerland, 1986), Vol. 10–12, p. 387.
[160]J. R. Wagner, J. J. Krebs, G. H. Stauss, and A. M. White, Solid State Commun. **36**, 15 (1980).
[161]U. Kaufmann, M. Baeumler, J. Windscheif, and W. Wilkening, Appl. Phys. Lett. **49**, 1254 (1986).
[162]M. Bauemler, U. Kaufmann, and J. Windscheif, in *Semi-Insulating III-V Materials*, edited by H. Kukimoto and S. Miyazawa (Ohmsha, North-Holland, Amsterdam, 1986), p. 361.
[163]T. Tsukada, T. Kikuta, and K. Ishida, Jpn. J. Appl. Phys. **24**, L689 (1985).
[164]M. Bauemler, U. Kaufmann, and J. Windscheif, Mater. Res. Soc. Symp. Proc. **46**, 201 (1985).
[165]H. J. von Bardeleben and J. C. Bourgoin, in *Semi-Insulating III-V Materials*, edited by H. Kukimoto and S. Miyazawa (Ohmsha, North-Holland, Amsterdam, 1986), p. 351.
[166]S. M. Eetemadi and R. Braunstein, J. Appl. Phys. **58**, 2217 (1985).
[167]E. W. Williams and H. B. Bebb, in *Semiconductors and Semimetals* (Academic, New York, 1972), Vol. 8, Chap. 5.
[168]B. Tuck, Phys. Status Solidi **29**, 793 (1968).
[169]L. J. Vieland and I. Kudman, J. Phys. Chem. Solids **24**, 437 (1963).
[170]C. J. Huang, Phys. Rev. **180**, 827 (1969).
[171]H. Kressel, F. Z. Hawrylo, and P. Le Fur, J. Appl. Phys. **39**, 4059 (1968).
[172]R. Williams, J. Appl. Phys. **37**, 3411 (1966).
[173]J. Blanc, R. H. Bube, and L. R. Weisberg, J. Phys. Chem. Solids **23**, 829 (1962).
[174]J. Blanc, R. H. Bube, and H. E. MacDonald, J. Appl. Phys. **32**, 1666 (1961).
[175]S. M. Sze and J. C. Irvin, Solid State Electron. **11**, 599 (1968).
[176]A. L. Lin, E. Omekanovski, and R. H. Bube, J. Appl. Phys. **47**, 1852 (1976).
[177]A. L. Lin and R. H. Bube, J. Appl. Phys. **47**, 1859 (1976).
[178]A. Mircea and A. Mitonneau, Appl. Phys. **8**, 15 (1975).
[179]G. Vincent and D. Bois, Solid State Commun. **27**, 431 (1978).
[180]D. Bois and G. Vincent, J. Phys. Lett. **38**, L351 (1977).
[181]G. Vincent, D. Bois, and A. Chantre, J. Appl. Phys. **53**, 3643 (1982).
[182]For a review, see G. Martin and S. Makram-Ebeid, in *Deep Centers in Semiconductors*, edited by S. T. Pantelides (Gordon & Breach, New York, 1986), p. 399.
[183]J. Lagowski and H. C. Gatos, in *Thirteenth International Conference on Defects in Semiconductors*, edited by L. C. Kimerling and J. M. Parsey (The Metallurgical Society of AIME, New York, 1985), p. 73.
[184]M. Kaminska, M. Skowronski, J. Lagowski, J. M. Parsey, and H. C. Gatos, Appl. Phys. Lett. **43**, 302 (1983).
[185]C. Hilsum and A. C. Rose-Innes, in *Semiconducting III-V Compounds* (Pergamon, New York, 1961), p. 142.
[186]G. M. Martin, G. Jacob, J. P. Hallais, F. Grainger, J. A. Roberts, J. B. Clegg, P. Blood, and G. Poiblaud, J. Phys. C **15**, 1841 (1982).
[187]A. M. Huber, N. T. Link, J. C. Debrun, M. Valladon, G. M. Martin, A. Mitonneau, and A. Mircea, J. Appl. Phys. **50**, 4022 (1979).
[188]R. H. Wallis, M. A. Di Forte-Poisson, M. Bonnet, G. Beuchet, and J. P. Duchemin, Inst. Phys. Conf. Ser. **56**, 73 (1981).
[189]E. R. Weber and J. Schneider, Physica **116B**, 398 (1983).
[190]E. R. Weber, H. Ennen, U. Kaufman, J. Windscheif, J. Schneider, and T. Wosinski, J. Appl. Phys. **53**, 6140 (1982).
[191]M. Kaminska, M. Skowronski, and W. Kuszko, Phys. Rev. Lett. **55**, 2204 (1985).
[192]T. Figielski, E. Kaczmarek, and T. Wosinski, Appl. Phys. **1**, 3177 (1985).
[193]J. Lagowski, H. C. Gatos, J. M. Parsey, K. Wada, M. Kaminska, and W. Walukiewicz, Appl. Phys. Lett. **40**, 342 (1982).
[194]G. A. Baraff and M. Schlüter, Phys. Rev. Lett. **55**, 2340 (1985).
[195]J. F. Wager and J. A. Van Vechten, Phys. Rev. B **35**, 2330 (1987).
[196]Z. Yuanxi, Inst. Phys. Conf. Ser. **63**, 185 (1982).
[197]J. Lagowski, M. Kaminska, J. M. Parsey, H. C. Gatos, and W. Walukiewicz, Inst. Phys. Conf. Ser. **65**, 41 (1983).
[198]H. J. von Bardeleben, D. Stiévenard, D. Deresmes, A. Huber, and J. C. Bourgoin, Phys. Rev. B **34**, 7192 (1986).
[199]B. K. Meyer, D. M. Hofmann, J. R. Niklas, and J. M. Spaeth, Phys. Rev. B **36**, 1332 (1987).
[200]B. K. Meyer, J. M. Spaeth, and M. Scheffler, Phys. Rev. Lett. **52**, 851 (1984).
[201]J. M. Spaeth, D. M. Hofmann, and B. K. Meyer, Mater. Res. Soc. Symp. Proc. **46**, 185 (1985).
[202]J. M. Spaeth, Annual Meeting of the Deutchen Physikalischen Gesellschaft (Freudenstadt, FRG, 1985) (unpublished).
[203]B. K. Meyer, D. M. Hofmann, and J. M. Spaeth, in *Defects in Semiconductors, Material Science Forum*, edited by H. J. von Bardeleben (Trans

Tech, Aedermannsdorf, Switzerland, 1986), Vol. 10–12, p. 311.
[204]J. M. Spaeth, in *Growth, Characterization, Processing of III-V Materials with Correlation to Device Performances*, edited by Y. I. Nissim and P. A. Glasow (Editions de Physique, France, 1987), p. 421.
[205]C. Delerue, M. Lannoo, D. Stiévenard, H. J. von Bardeleben, and J. C. Bourgoin, Phys. Rev. Lett. **59**, 2875 (1987).
[206]H. J. von Bardeleben, J. C. Bourgoin, D. Stiévenard, and M. Lannoo, *GaAs and Related Compounds 1987*, Inst. Phys. Conf. Ser. No. 91 (Institute of Physics, London, 1988), p. 399.
[207]S. Makram-Ebeid, in *Defects in Semiconductors*, edited by J. Narayan and T. Y. Tan (North-Holland, New York, 1981), p. 495.
[208]S. Makram-Ebeid and M. Lannoo, Phys. Rev. B **25**, 6406 (1982).
[209]A. Mircea, A. Mitonneau, L. Hollan, and A. Brière, Appl. Phys. **11**, 153 (1976).
[210]W. Walukiewicz, J. Lagowski, and H. C. Gatos, Appl. Phys. Lett. **43**, 112 (1983).
[211]T. Wosinski, Appl. Phys. A **36**, 213 (1985).
[212]J. Lagowski, D. G. Lin, T. P. Chen, M. Skowronski, and H. C. Gatos, Appl. Phys. Lett. **47**, 929 (1985).
[213]J. Osaka, H. Okamoto, and K. Kobayashi, in *Semi-Insulating III-V Materials* (Ohmsha, North-Holland, Amsterdam, 1986), p. 421.
[214]A. Bencherifa, G. Brémond, A. Nouilhat, G. Guillot, A. Quivarch, and A. Regreny, Rev. Phys. Appl. **22**, 891 (1987).
[215]G. M. Martin, Appl. Phys. Lett. **39**, 747 (1981).
[216]H. Nakashima, M. Matsunaya, and Y. Shiraki, Inst. Phys. Conf. Ser. **63**, 203 (1982).
[217]P. Leyral, G. Vincent, A. Nouilhat, and G. Guillot, Solid State Commun. **42**, 67 (1982).
[218]D. R. Wright, I. D. Blenkinsop, and S. J. Bass, in *Semi-Insulating III-V Materials*, edited by G. J. Rhees (Shiva, Nantwich, 1980), p. 174.
[219]B. V. Shanabrook, P. B. Klein, E. M. Swiggard, and S. G. Bishop, J. Appl. Phys. **54**, 336 (1983).
[220]P. W. Yu, D. E. Holmes, and R. T. Chen, Int. Phys. Conf. Ser. **63**, 200 (1982).
[221]P. W. Yu, Solid State Commun. **43**, 953 (1982).
[222]A. Mircea-Roussel and S. Makram-Ebeid, Appl. Phys. Lett. **38**, 1007 (1981).
[223]P. Leyral and G. Guillot, in *Semi-Insulating III-V Materials*, edited by S. Makram-Ebeid and B. Tuck (Shiva, Nantwich, 1982), p. 166.
[224]M. Tajima, Jpn. J. Appl. Phys. **26**, L885 (1987).
[225]L. Samuelson, P. Omling, and H. G. Grimmeis, Appl. Phys. Lett. **45**, 521 (1984).
[226]D. E. Holmes, R. T. Chen, K. R. Elliott, C. G. Kirkpatrick, and P. W. Yu, IEEE Trans Electron Devices **ED-29**, 1045 (1982).
[227]D. E. Holmes, R. T. Chen, K. R. Elliott, and C. G. Kirkpatrick, Appl. Phys. Lett. **40**, 46 (1982).
[228]D. E. Holmes, K. R. Elliott, R. T. Chen, and C. G. Kirkpatrick, in *Semi-Insulating III-V Materials*, edited by S. Makram-Ebeid and B. Tuck (Shiva, Nantwich, 1982), p. 19.
[229]E. E. Wagner, D. E. Mars, G. Hom, and G. B. Stringfellow, J. Appl. Phys. **51**, 5434 (1980).
[230]L. Samuelson, P. Omling, H. Titze, and H. G. Grimmeis, J. Cryst. Growth **55**, 164 (1981).
[231]M. O. Watanabe, A. Tanaka, T. Nakanisi, and Y. Zohta, Jpn. J. Appl. Phys. **20**, L429 (1981).
[232]M. Kaminska, M. Skowronski, J. Lagowski, J. M. Parsey, and H. C. Gatos, Appl. Phys. Lett. **43**, 302 (1983).
[233]M. O. Manasreh and B. C. Covington, Phys. Rev. B **36**, 2730 (1987).
[234]A. Mitonneau and A. Mircea, Solid State Commun. **30**, 157 (1979).
[235]S. Nojima, J. Appl. Phys. **57**, 620 (1985).
[236]Y. Mochizuki and T. Ikoma, Jpn. J. Appl. Phys. **24**, L895 (1985).
[237]J. C. Parker and R. Bray, in *Defects in Semiconductors, Material Science Forum*, edited by H. J. von Bardeleben (Trans Tech, Aedermannsdorf, Switzerland, 1986), Vol. 10–12, p. 347.
[238]D. W. Fischer, Appl. Phys. Lett. **50**, 1751 (1987).
[239]H. J. von Bardeleben, N. T. Bagraev, and J. C. Bourgoin, Appl. Phys. Lett. **51**, 1451 (1987).
[240]M. Baeumler, U. Kaufmann, and J. Windscheif, Appl. Phys. Lett. **46**, 781 (1985).
[241]Y. Mochizuki and T. Ikoma, in *Defects in Semiconductors, Material Science Forum*, edited by H. J. von Bardeleben (Trans. Tech, Aedermannsdorf, Switzerland, 1986), Vol. 10–12, p. 323.
[242]T. Figielski and T. Wosinski, Phys. Rev. B **36**, 1269 (1987).
[243]M. Levinson and J. A. Kafalas, Phys. Rev. B **35**, 9383 (1987).
[244]D. Stiévenard, H. J. von Bardeleben, J. C. Bourgoin, and A. Huber, in *Defects in Semiconductors, Material Science Forum*, edited by H. J. von Bardeleben (Trans Tech, Aedermannsdorf, Switzerland, 1986), Vol. 10–12, p. 305.
[245]J. C. Bourgoin and M. Lannoo, Rev. Phys. Appl. **23**, 863 (1988).
[246]G. A. Baraff and M. Lannoo, Rev. Phys. Appl. **23**, 817 (1988).
[247]G. A. Baraff, M. Lannoo, and M. Schlüter, Proceedings of the Fall Meeting of the MRS, Boston, Dec. 1987 (unpublished).
[248]G. A. Baraff and M. Schlüter, Phys. Rev. B **35**, 6154 (1987).
[249]For a discussion, see J. W. Corbett and J. C. Bourgoin, in *Point Defects in Solids*, edited by J. H. Crawford and L. M. Slifkin (Plenum, New York, 1975), Vol. 2, Chap. 1.
[250]R. Carr, P. J. Kelly, A. Oshiyama, and S. T. Pantelides, in *Thirteenth International Conference on Defects in Semiconductors*, edited L. C. Kimerling and J. M. Parsey (The Metallurgical Society of AIME, New York, 1985), p. 269.
[251]Y. Bar-Yam and J. D. Joannopoulos, in *Thirteenth International Conference on Defects in Semiconductors*, edited by L. C. Kimerling and J. M. Parsey (The Metallurgical Society of AIME, New York, 1985), p. 261.
[252]G. A. Baraff and M. Schlüter, Phys. Rev. Lett. **55**, 1327 (1985).
[253]C. Song, W. Ge, D. Jiang, and C. Hsu, Appl. Phys. Lett. **50**, 1666 (1987).
[254]X. Zhong, D. Jiang, W. Ge, and C. Song, Appl. Phys. Lett. **52**, 628 (1988).
[255]J. Dabrowski and M. Scheffler Phys. Rev. Lett. **60**, 2183 (1988).
[256]D. J. Chadi and K. J. Chang Phys. Rev. Lett. **60**, 2187 (1988).
[257]T. Figielski and T. Wosinski, Phys. Rev. B **36**, 1269 (1987).
[258]Y. Mochizuki and T. Ikoma, Rev. Phys. Appl. **23**, 767 (1988).
[259]H. J. von Bardeleben, D. Stiévenard, and J. C. Bourgoin, in *Proceedings of the 15th International Conference on Defects in Semiconductors*, Budapest, 1988 (to be published).
[260]J. P. Fillard, M. Castagné, J. Bonnafé, and M. de Mureca, J. Appl. Phys. **54**, 6767 (1983).
[261]J. A. Van Vechten, J. Electrochem. Soc. **122**, 423 (1975).
[262]B. V. Shanabrook, P. B. Klein, and S. G. Bishop, Physica **117B+118B**, 173 (1983).
[263]T. Figielski, Appl. Phys. A **35**, 255 (1984).
[264]D. C. Look, P. W. Yu, W. M. Theis, W. Ford, G. Mathur, J. R. Sizelove, D. H. Lee, and S. S. Li, Appl. Phys. Lett. **49**, 1083 (1986).
[265]D. C. Look, W. M. Theis, P. W. Yu, J. R. Sizelove, W. Ford, and G. Mathar, J. Electron. Mater. **16**, 63 (1987).
[266]J. Lagowski, H. C. Gatos, C. H. Kang, M. Skowronski, K. Y. Ko, and D. G. Lin, Appl. Phys. Lett. **49**, 892 (1986).
[267]H. Steinbardt and P. Haasen, Phys. Status Solidi A **49**, 93 (1978).
[268]P. Haasen, Phys. Status Solidi A **28**, 145 (1975).
[269]N. Nakata and T. Ninomiya, J. Phys. Soc. Jpn. **42**, 552 (1977).
[270]S. Miyazawa, Y. Ishii, S. Ishida, and Y. Naniski, Appl. Phys. Lett. **43**, 853 (1985).
[271]A. K. Chin, R. Caruso, M. S. S. Young, and A. R. von Neida, Appl. Phys. Lett. **45**, 552 (1984).
[272]A. K. Chin, I. Camlibel, R. Caruso, M. S. S. Young, and A. R. von Neida, J. Appl. Phys. **57**, 2203 (1985).
[273]B. Wakefield, P. A. Leigh, M. H. Lyons, and C. K. Elliott, Appl. Phys. Lett. **45**, 66 (1984).
[274]H. J. Hovel and D. Gindotti, IEEE Trans. Electron Devices **ED-32**, 2331 (1985).
[275]I. Fujimoto, Jpn. J. Appl. Phys. **23**, L287 (1984).
[276]D. J. Stirland, Inst. Phys. Conf. Ser. **33a**, 150 (1977).
[277]P. D. Augustus and D. J. Stirland, J. Microsc. **118**, 111 (1980).
[278]A. G. Cullis, P. D. Augustus, and D. J. Stirland, J. Appl. Phys. **51**, 2556 (1980).
[279]P. Petroff, Inst. Phys. Conf. Ser. **23**, 73 (1975).
[280]J. Ding, J. S. C. Chang, and M. Bujatti, Appl. Phys. Lett. **50**, 1089 (1987).
[281]S. Miyazawa and F. Hyuga, IEEE Trans. Electron. Devices **ED-33**, 227 (1986).
[282]S. Miyazawa and K. Wada, Appl. Phys. Lett. **48**, 905 (1986).
[283]J. Marek, A. G. Elliott, V. Wilke, and R. Geiss, Appl. Phys. Lett. **49**, 1732 (1986).
[284]W. Heinke and H. J. Queisser, Phys. Rev. Lett. **33**, 1082 (1974).
[285]W. Heinke, Inst. Phys. Conf. Ser. **23**, 380 (1975).
[286]A. T. Hunter, Appl. Phys. Lett. **47**, 715 (1985).
[287]D. L. Barett, S. McQuigan, H. M. Holgood, G. W. Elredge, and R. N. Thomas, J. Cryst. Growth **70**, 179 (1984).
[288]D. E. Holmes and R. T. Chen, J. Appl. Phys. **55**, 3588 (1984).

[289]D. E. Holmes, R. T. Chen, K. R. Elliott, and C. G. Kirkpatrick, Appl. Phys. Lett. **43**, 305 (1983).
[290]M. S. Skolnick, I. J. Reed, and A. D. Pitt, Appl. Phys. Lett. **44**, 447 (1984).
[291]W. Wettling and J. Windscheif, Appl. Phys. A **40**, 191 (1986).
[292]F. A. Ponce, F. C. Wang, and R. Hiskes, in *Semi-Insulating III-V Materials*, edited by D. C. Look and J. S. Blakemore (Shiva, Nantwich, 1984), p. 68.
[293]F. A. Ponce, Inst. Phys. Conf. Ser. **76**, 1 (1985).
[294]J. Osaka, F. Hyuga, and K. Watanabe, Appl. Phys. Lett. **47**, 1307 (1985).
[295]B. Pödör, J. Appl. Phys. **55**, 3603 (1984).
[296]P. Dansas, J. Appl. Phys. **58**, 2212 (1985).
[297]D. C. Look and G. S. Pomrenke, J. Appl. Phys. **54**, 3249 (1983).
[298]T. Hiramoto, Y. Mochizuki, and T. Ikoma, Jpn. J. Appl. Phys. **25**, L830 (1986).
[299]P. Alnot, D. Vuillaume, and J. C. Bourgoin (unpublished).
[300]S. Makram-Ebeid, D. Gautard, P. Devillard, and G. M. Martin, Appl. Phys. Lett. **40**, 161 (1982).
[301]S. Y. Chiang and G. L. Pearson, J. Appl. Phys. **46**, 2986 (1975).
[302]D. J. Stirland, M. R. Brozel, and I. Grant, Appl. Phys. Lett. **46**, 1066 (1985).
[303]M. R. Brozel, I. Grant, R. M. Ware, and D. J. Stirland, Appl. Phys. Lett. **42**, 610 (1983).
[304]H. J. von Bardeleben, J. C. Bourgoin, and H. R. Zelsmann, in *Growth, Characterization, Processing of III-V Materials with Correlations to Device Performances*, edited by Y. I. Nissim and P. A. Glasow (Les Editions de Physique, France, 1987), p. 451.
[305]A. K. Jonscher, in *Electronic and Structural Properties of Amorphous Semiconductors*, edited by P. Le Comber and J. Mort (Academic, New York, 1973), p. 329.
[306]B. Pistoulet, P. Girard, and G. Hamamdjian, J. Appl. Phys. **56**, 2268 (1984).
[307]B. Pistoulet, P. Girard, and G. Hamamdjian, J. Appl. Phys. **56**, 2275 (1984).
[308]B. Pistoulet, F. M. Roche, and S. Abdalla, Phys. Rev. B **30**, 5987 (1984).
[309]B. Pistoulet and G. Hamamdjian, Phys. Rev. B **35**, 6305 (1987).
[310]S. Abdalla and B. Pistoulet, J. Appl. Phys. **58**, 2646 (1985).
[311]A. K. Jonscher, C. Pickup, and S. H. Zaidi, Semicond. Sci. Technol. **1**, 71 (1986).
[312]S. Miyazawa, T. Honda, Y. Ishii, and S. Ishida, Appl. Phys. Lett. **44**, 410 (1984).